

COMPONENTS OF OCEANIC SEA-LEVEL PRESSURE AND THEIR
RELATIONSHIP WITH RAINFALL OVER SOUTHERN AFRICA

CAROLANN HOWES

A thesis submitted to the Faculty of Science,
University of the Witwatersrand, Johannesburg,
for the degree of Master of Science.

Johannesburg, 1980

This is to declare that this
thesis is entirely my own work
and has not been previously
submitted as a thesis for any
degree in any other university.

Howes.

*This dissertation is dedicated
to Charles and Elizabeth Howes*

- 1 -

ABSTRACT

Monthly mean sea-level pressure over the oceanic areas adjacent to the Republic of South Africa is analysed. Relationships between the oceanic pressure and rainfall over this part of the continent are discussed. Principal components analysis is used to derive uncorrelated functions of the original pressure variables. Three major pressure fields were identified, termed a general, a longitudinal and a latitudinal pressure field. The relationships between pressure and rainfall are assessed by regressing monthly rainfall on the principal component scores. Rainfall in winter maxima areas appears to be directly related to oceanic sea-level pressure situations, whereas the rest of the country shows an out-of-season relationship between rainfall and pressure over non-continental areas.

PREFACE

Atmospheric circulation over the northern hemisphere has been well documented, unlike that over the southern hemisphere. The lack of detailed knowledge concerning annual, seasonal and monthly variations in the atmospheric circulation may be attributed, in part, to difficulties in obtaining data over the large oceanic areas that are characteristic of the southern hemisphere.

Whereas circulation over the subcontinent is well understood and has been for many years, the same cannot be said for the situation surrounding southern Africa. The region lies astride the subtropical high pressure belt, with the Atlantic Ocean high to the west and the Indian Ocean high to the east. Southwards is the low pressure trough associated with the westerly circulation. Little work has been done to define the interacting components of sea-level pressure over the oceans surrounding the coasts of southern Africa.

In order to provide further information the following hypothesis is investigated in this dissertation: that changes in the oceanic pressure fields surrounding the African subcontinent, and their components, are of importance in specifying the manner in which moisture is transported into circulation

systems prevailing over the continental area. More specifically, the objectives of the dissertation are:

- (i) to conduct an analysis of monthly sea-level pressure over the oceans adjacent to southern Africa using principal components analysis, and
- (ii) to investigate the link between the derived oceanic pressure components and rainfall over the subcontinent.

The actual methods of moisture transportation and the precipitation-producing mechanisms over the subcontinent will not be considered in the study.

In Chapter 1 an historical background and a review of southern hemispheric circulation patterns is presented, with special note of principal component studies of pressure analyses. Pressure data and the method of analysis used to illustrate the component pressure patterns as well as rainfall data and the technique used to investigate relationships between rainfall over the Republic and pressure are described in Chapter 2. The following three chapters presents the results of the analysis of pressure data. Chapter 6 discusses both detailed and general interrelationships between oceanic sea-level pressure and rainfall over South Africa. Concluding remarks are presented in Chapter 7.

Mr P Stickler was responsible for the final form of the diagram. To him, and to the staff of the Computer Center - University of the Witwatersrand, I extend my thanks for their willing assistance.

I stand much in the debt of my family, who must be thanked for their consistent encouragement; my mother who gave invaluable assistance with proof reading; and my sister, Vivienne, for the many hours spent computer punching and helping prepare the diagrams.

Dr T G J Dyer, my supervisor, must be acknowledged as the person who first introduced me to statistical climatology. I extend my warmest thanks to him for his stimulating discussion and ready advice during the course of this research.

Gratitude is expressed to Professor P D Tyson, who, in the absence of Dr Dyer, supervised the final drafting of this dissertation. Particular thanks are expressed for the time he devoted to providing helpful criticisms and consistent encouragement.

The research was financed by a grant from the Richard Ward Endowment Fund.

CONTENTS

Chapter 1 HISTORICAL BACKGROUND

1.1	Introduction	1
1.2	Aspects of southern hemispheric circulation	4
1.3	Principal components analysis of pressure fields	7

Chapter 2 DATA AND METHODS OF ANALYSIS

2.1	Introduction	13
2.2	Oceanic sea-level atmospheric pressure	13
2.3	Principal components analysis	14
2.4	Rainfall data	17
2.5	Stepwise multiple regression	18

Chapter 3 MEAN PRESSURE PATTERNS AND THE GENERAL PRESSURE FIELD

3.1	Introduction	20
3.2	Mean monthly pressure patterns	20
3.3	Pressure fields	24
3.4	The general pressure field	26

3.5	Seasonal changes in the general pressure field	27
	Summer conditions	27
	The winter pattern	31
	Transition periods	31
3.6	Temporal variation of the general pressure fields	34
3.7	Discussion	37

Chapter 4 THE LONGITUDINAL PRESSURE FIELD

4.1	Introduction	40
4.2	Seasonal changes in the longitudinal pressure field	42
	Summer conditions	42
	The winter pattern	42
4.3	Temporal variation of the longitudinal pressure fields	44
4.4	Discussion	48

Chapter 5 THE LATITUDINAL PRESSURE FIELD

5.1	Introduction	51
5.2	Seasonal changes in the latitudinal pressure field	53
	Late summer conditions	53
	Late winter conditions	53
5.3	Temporal variation of the latitudinal pressure fields	56
5.4	Discussion	56

Chapter 6 RELATIONSHIPS BETWEEN OCEANIC SEA-LEVEL PRESSURE AND RAINFALL

6.1	Introduction	60
-----	---------------------	----

6.2	Annual march of rainfall over South Africa	60
6.3	The regression analysis	62
	Low restriction analysis					62
	Rainfall relationships with the general pressure field					63
	Rainfall relationships with the longitudinal pressure field					63
	Rainfall relationships with the latitudinal pressure field					66
	High restriction analysis					66
6.4	Seasonal dependence of rainfall pressure interactions	75
6.5	Discussion	77
Chapter 7	CONCLUSION	79
References	83
Appendix 1	Mean monthly pressure charts	90
Appendix 2	Mean monthly temperature charts	94
Appendix 3	General pressure field and R^2 contours for rainfall	98
Appendix 4	Longitudinal pressure field and R^2 contours for rainfall	102
Appendix 5	Latitudinal pressure field and R^2 contours for rainfall	106
Appendix 6	Regression equations	110
Appendix 7	Principal components entered into regression equations	119

CHAPTER 1

HISTORICAL BACKGROUND

1.1 INTRODUCTION

A large amount of work has been carried out to determine the nature of the general circulation of the northern hemisphere and it can be fairly claimed that this is now well understood. Reviews of Northern Hemispheric circulation patterns may be found in Palmen and Newton (1969) and Barry and Perry (1973). Fewer advances have been made in understanding the circulation of the Southern Hemisphere, owing to a paucity of data, particularly over the oceanic areas. The IGY (1957/58) provided much additional data concerning circulation within the hemisphere (for example Taljaard 1966, 1967, 1969; van Loon 1964, 1965, 1967). This knowledge has been augmented by the International Southern Hemisphere Drifting Bouy program of the WMO.

Over the subcontinent of southern Africa, mean circulation patterns are well understood as a result of the work of Jackson (1947, 1952), Taljaard (1953), Rubin (1956) and others. Throughout the year, the mean circulation pattern is anticyclonic,

is stronger in winter than in summer, and is displaced northwards during the winter. The link between mean circulation patterns and the occurrence of rainfall is not always good. On a daily scale, circulation and precipitation are well understood following Longley's application of Lund's technique (Lund, 1962) for developing a typology of synoptic types for South Africa (Longley, 1976).

Descriptions of the atmospheric circulation over the adjacent oceans are only to be found in general works relating to the hemisphere as a whole (for example Vowinkel 1953; Newton *et al.* 1972; Taljaard 1966, 1969; van Loon 1965, 1967b; Taljaard & van Loon, 1960, 1964). South Africa lies astride the subtropical high pressure belt which affects the whole of the southern hemisphere (Fig 1.1). Anticyclones occur to the west of the subcontinent, the South Atlantic Ocean high (referred to as the Atlantic Ocean high) and to the



Fig 1.1 Southern Africa

east the Indian Ocean high. Mean pressure in the Indian Ocean high is generally lower than that over the Atlantic Ocean high. To the south pressure variability increases towards the low pressure belt associated with the westerlies. Although detailed analysis of the seasonal variation of the harmonic components of the mean atmospheric circulation are well documented (van Loon 1967a; van Loon & Jenne, 1972), seasonal variations in the circulation pattern *per se* are not well understood. It is also not known how these different components of pressure interact or how they can be separated over the oceanic areas.

The aim of this dissertation is, in the first instance, to conduct an analysis of monthly sea-level pressure over the oceans adjacent to southern Africa for the period 1951 - 1970. Principal components analysis will be used to determine components of the oceanic pressure field and their spatial and temporal variations. Secondly, the link between the derived components of the surface pressure field and rainfall over the subcontinent will be assessed.

In so doing the following hypothesis is examined: that changes in the oceanic pressure fields, and their components, are of importance in specifying the manner in which moisture is transported into circulation systems prevailing over the continental area. Whereas the general circulation over the oceans adjacent to South Africa exerts strong indirect control

on weather and climate, it is the actual systems prevailing over the subcontinent that produce the direct controls of the precipitation patterns that prevail. For this reason it is to be expected that no strong correlation between derived oceanic pressure parameters and rainfall over the Republic will be evident. The actual precipitation-producing mechanisms over the subcontinent of southern Africa will not be considered.

1.2 ASPECTS OF SOUTHERN HEMISPHERIC CIRCULATION

In 1869 Buchan published maps showing the mean sea-level pressure distribution of the southern hemisphere. de Bort (1893) produced the first upper air charts for this hemisphere, extrapolating pressure values up to 4 km. First monthly mean charts of sea-level circulation patterns south of 30° were constructed by Meinardus and Mecking (1911). Other studies of pressure patterns on the southern hemisphere were carried out by Meinardus (1928, 1929), Wahl (1942), Palmer (1942), Volinckel (1955) and Schwerdtfeger and Prohaska (1956). Observations made during the IGY have done much to expand hemispheric knowledge (for example, Taljaard 1966, van Loon 1965, 1967). A brief outline of current knowledge of atmospheric circulation in the southern hemisphere follows.

Atmospheric circulation patterns of the southern hemisphere may be divided into zonal and meridional features, (Fig 1.2).

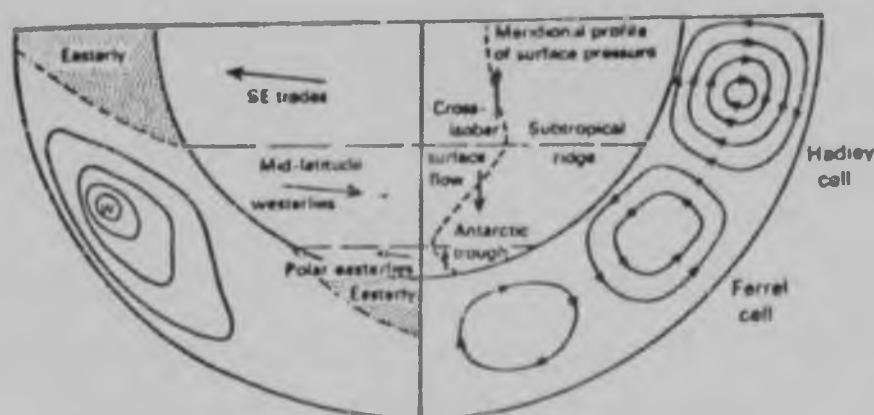


Fig 1.2 Schematic representation of the principal features of the general circulation for the Southern Hemisphere showing the meridional circulation (right) and zonal circulation (left). (Pittcock (1978)).

These circulations may be summarised as follows:

- (i) a shallow belt of polar easterlies extending equatorward to about 65° latitude at the surface but varying with the seasons;
- (ii) a broad band of mid latitude westerlies increasing with height to a maximum which is strongest (greater than 40 m s^{-1}) and at its lowest latitude (around 30°) in winter;
- (iii) a zone of Trade-Wind easterlies separated from the westerlies by subtropical ridges which slope equatorward with height from around 30° at the surface to about 10° at 200 mb;
- (iv) a three-cell mean meridional circulation with ascending motion in the equatorial belt and around latitude 60° and with descent over the poles and in the vicinity of latitude 30° (Pittcock, 1978).

The subtropical high pressure belt is found between 23° - 42° S and is centred around 30° S. At sea-level, the belt exhibits a series of quasi-permanent anticyclones, separated from each other by continental masses. Equatorwards, the anticyclonic circulation results in the equatorial easterlies. To the south, westerlies develop. Subtropical anticyclones weaken with increasing altitude, eventually disappearing. Seasonal variations result in both zonal and meridional movement of these anticyclones.

The tropospheric circumpolar vortex dominates circulation patterns south of the subtropical highs. The vortex consists of strong westerly winds which reach their maximum velocities in the upper troposphere and which contain trains of travelling cyclones and anticyclones (Lamb, 1959). Cores of strong westerlies, the subtropical jet streams, are found at 10 - 15 km and characterise a sharp poleward temperature decrease in the troposphere (Tucker, 1978). The circumpolar vortex is not entirely symmetrical around the south pole, owing to the irregular distribution of oceanic and land masses.

As is characteristic of the northern hemisphere, 3 mean zonal standing waves characterise the circumpolar vortex in the southern hemisphere (van Loon and Jenne, 1972). These waves are less well developed than their counterparts in the northern hemisphere, owing to fewer land masses. Zonal wave 1

defines the eccentricity of the circumpolar vortex and shows a ridge in the subtropical Atlantic Ocean and a trough in the Pacific region. Wave 2 has a large standing component over Antarctica. In all months, wave 3 is well defined between 25° S and 60° S [Fig 1.3].

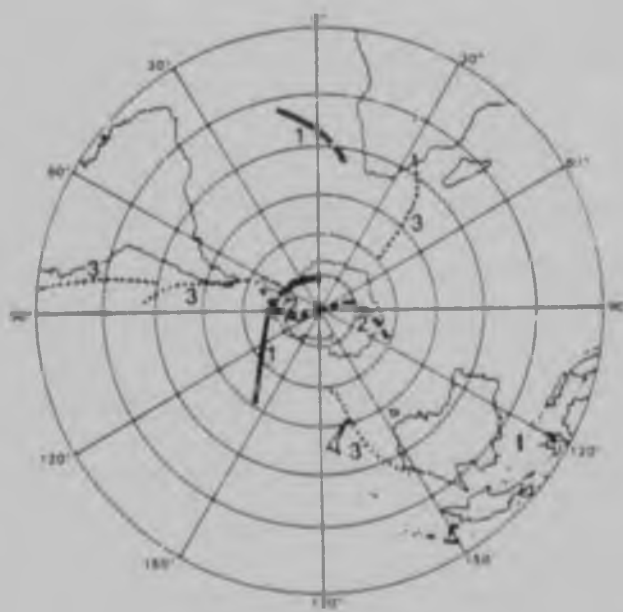


Fig 1.3 The position of the ridges of standing waves 1, 2 and 3 in the annual mean 500 mb map, and of wave 3 at 200 mb in January. (van Loon & Jenne, 1972)

1.3 PRINCIPAL COMPONENTS ANALYSIS OF PRESSURE FIELDS

Principal components (also known as eigenvectors or empirical orthogonal functions) have been used in many studies of atmospheric pressure and other related meteorological parameters.

- 8 -

In an early study Das (1956) employed monthly sea-level pressure data from 9 stations down the east coast of Australia to investigate the intensity and position of the subtropical high belt. Orthogonal polynomials (the forerunner of principal components analysis) combined with tests for serial correlation, showed that the belt moved slowly southward during the period 1909 to 1954.

Veitch (1965) used principal components analysis to describe daily mean sea-level pressure values for the Australasian area. In addition to confirming the eastward succession of mid-latitude cyclones and anticyclones and the oscillation of zonal pressure indices, he was able to show that an important source of pressure variability was a quasi-periodic oscillation of 10 to 40 days over eastern Australia.

In a somewhat different study, Trenberth (1975) investigated monthly mean sea-level pressure anomalies and monthly sea surface temperature deviations from the normal. In a later extension to his work, Trenberth (1976) used the results of the principal components analysis to derive general circulation indices for the Australasian area. Maps of the principal component scores represented sea-level pressure anomaly patterns over time. Regimes of weather were investigated by linking derived indices with indices of zonal and meridional airflow. The time series of the principal components were used to show that whereas the first two pressure anomaly

patterns appeared to affect weather regimes, precipitation is poorly correlated with these.

Examples of other principal component studies in which relationships between pressure and variables such as temperature, wind speed and direction are discussed, are to be found in the work of Winstanley (1973), Haworth (1978), Kidson (1975a) and Kutzbach (1967, 1970).

Winstanley (1973) related fluctuations to changes in the rainfall patterns of the Middle East, Sahel zone and Mediterranean area to changes in the general circulation of the atmosphere. The zonal circulation over the northern hemisphere was found to be of great importance in regulating precipitation in these areas.

Using principal components analysis, Haworth (1978) conducted an analysis of surface pressure anomalies combined with sea surface temperature anomalies. In most months of the year, variations in sea surface temperature in the tropical east Atlantic were shown to be related to the surface pressure distribution. Long term changes in the sea surface temperature in this area were related to variations in sea-level pressure in the higher latitudes.

Kidson (1975a) examined the relationship between monthly

means of surface pressure, temperature and rainfall by using principal components to analyse their hemispheric data matrix in both hemispheres. Results showed that rainfall components were of a regional nature, whereas temperature and pressure showed hemispheric coherence.

Groups of monthly mean sea-level pressure, surface temperature and precipitation over North America were related (Kutzbach 1967, 1970). In the first study, emphasis was laid on principal components analysis of the three variables for this region, the structure of the covariances between them being confirmed by reference to actual synoptic situations. In the second study, data from January and July mean monthly sea-level maps were used in a principal components analysis to define spatial patterns of circulation variability over the northern hemisphere. The first few eigenvectors described the major circulation features within the atmosphere, such as the winter Siberian high, the summer Asiatic low and the subtropical high pressure centres. Time series analysis of the principal component scores identified the early to mid-1920's and early to mid-1950's as periods of climatic change in hemispheric circulation which were associated with changes in the positions of large scale features of the general circulation.

Recently, Walsh & Mostek (1980) completed an eigenvector analysis of surface temperature, precipitation and sea-level

pressure over the United States. Derived anomaly patterns showed that large percentages of variance were accounted for by the first three principal components of each parameter. Cross correlations between the amplitudes of the eigenvectors are statistically significant and often seasonally dependent.

Examples of upper air pressure data analysis are found in the work of Craddock and Flood (1969) and Craddock and Flintoff (1969). Daily grid point data were extracted from hemispheric synoptic charts. A set of principal components were derived representing large-scale features of the height of the 500 mb surface over the Northern Hemisphere. Each resultant eigenvector was discussed as a feature of the general 500 mb surface circulation. For example Eigenvector 1 accounting for 58.6% of the total variance in the pressure data, was a general field devoid of strong gradients. Eigenvector 2 (3.4%) indicated the vortex over Greenland, whereas Eigenvector 3 (2.9%) corresponded to the Aleutian high. More recent work on the 500 mb level was carried out by Rinne and Karhila (1979) and Rinne and Jarvenaja (1979). In the first work, empirical orthogonal functions (principal components) were determined for the northern hemisphere to describe the 500 mb level. The second presented a study of the effectiveness of the components previously derived, the results indicating that the method used was stable over time and that the very large data matrix had been reliably reduced to 175 principal components. The work of Craddock and Flood (1969) and Craddock and Flintoff (1969) emphasised

the actual physical features whereas that of Rinne and Jarvenaja (1979) discussed the technique in depth and investigated its reliability.

Steyaert *et al* (1978) studied atmospheric pressure and its relationship to wheat yields in the United States, Canada and the Soviet Union. Principal component analysis was used to represent the large scale atmospheric features which, in turn, were then used as predictors in a linear regression analysis on wheat yields. A wheat yield model with high operational significance was provided which explained over 90% of the total variance in wheat production, the model providing estimates within two quintals per hectare of the official estimates for 1975 and 1976. Similar results were obtained from an analysis of maize production over southern Africa and sea-level pressure over the Indian and South Atlantic Oceans (Gillooly & Dyer, 1980).

Principal components analysis will be used in this study to decompose oceanic sea-level pressure data into component parts by deriving uncorrelated pressure fields. The amount of data to be considered is reduced and all variables are rendered uncorrelated. Details of the technique to be used are considered in the next chapter.

CHAPTER 2

DATA AND METHODS OF ANALYSIS

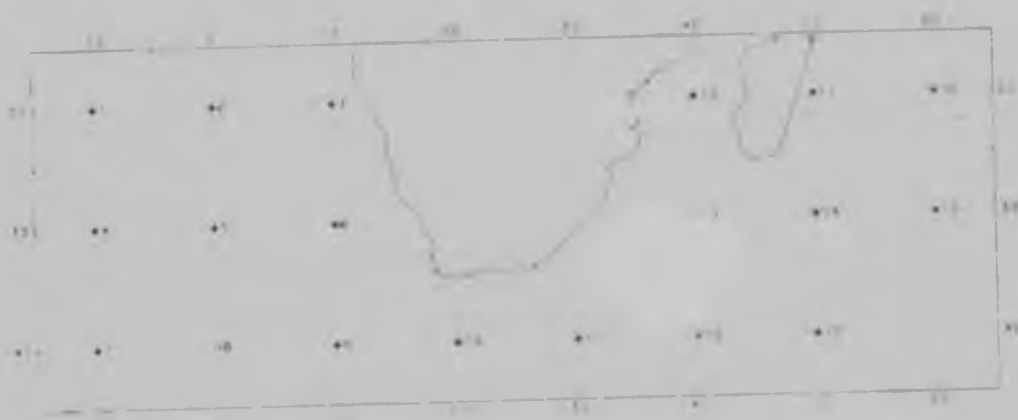
2.1 INTRODUCTION

Sea-level atmospheric pressure data for the oceans surrounding southern Africa are available at equally spaced, 10° latitude and longitude grid points over an area of ocean defined by 10° W to 60° E and 20° S to 40° S. Principal components analysis will be employed to derive pressure fields from the actual pressure data matrix and to ensure that the resulting fields are uncorrelated. The time series scores from the principal components analysis will be correlated with rainfall data from twenty district rainfall regions over the Republic of South Africa, using stepwise multiple regression. In this chapter the data and methods of analysis are discussed.

2.2 OCEANIC SEA-LEVEL ATMOSPHERIC PRESSURE

Sea-level pressure data at 19 grid points over the oceans surrounding southern Africa are described in the analysis (Fig 2.1). Monthly mean values for each grid point for the period 1951 to 1977 are used. Consequently, the

analysis of pressure data is based on 12 individual matrices being of order 27×19 , where rows are years and columns grid point, data being presented in whole mbs. Data were obtained from the South African Weather Bureau.



Grid points used for sea-level oceanic pressure data.

PRINCIPAL COMPONENTS ANALYSIS

Uncorrelated pressure fields have been derived from the total pressure data matrix using principal components analysis. The method of approach has two important characteristics: first, it usually reduces the dimension of the data matrix that needs be finally considered; secondly, it shows more clearly the interrelationships with the original data matrix (Maxwell, 1977).

Principal components analysis provides a mathematical reorganization of the original data matrix. The new variables, principal components, are uncorrelated linear functions

of the original variables. The total number of variables remains unchanged and the total variance of the data set is retained. However, the principal components are so derived that the greatest proportion of the total variance, obtainable by such a linear combination, in the data matrix is accounted for by the first component, the next largest amount by the second, and so on. Consequently the order in which they are formed is related to the proportion of total variance for which they account. Thus only those components accounting for most of the variance need be considered. Often the first few principal components account for a large proportion of the total variance, reducing the dimensionality of the problem (for example, Craddock, 1973; Kendall, 1975).

The pressure data used in this study, where a high degree of intercorrelation exists between the variables is well suited to principal components analysis. If little intercorrelation existed, it would be pointless to attempt to derive uncorrelated linear combinations since most components would then represent individual variables only.

The analysis has been based on the correlation matrix which reduces all the variables to equal importance as measured by scale, since large scale patterns were sought as opposed to more localised effects. Because the variables are standardized when using the correlation matrix, the

local variation is removed by virtue of having divided each variable by its standard deviation. Eigenvectors have been extracted from the correlation matrix for the pressure data matrix of individual months. Principal component scores of the original data matrix were calculated and plotted, as were loading values, or the coefficients of the linear function which the eigenvectors define (Davis, 1973). Because of the ambiguities that are present in the literature, it is well to define certain expressions used in principal components analysis. First, the elements of an eigenvector matrix are scaled (Maxwell, 1977) and are termed eigenvector loadings, or simply loadings. These loadings provide the value of the correlation between each variable and the respective principal component. The component scores are the same as the term component amplitudes, or coefficients sometimes seen in the literature. In the present work, loadings are on grid points, and scores form time series of pressure anomalies. A cut-off value of 1.0 was used for the eigenvalues, this being Kaiser's criterion (Child, 1970), to determine the importance of the patterns obtained from the above analysis. Rinne and Karhila (1979) indicated that whereas most of the variance is explained by the first few components, high-indexed tail components describe noise and errors of the original data. For this study the individual components soon accounted for minute amounts of variance only, as well as becoming extremely difficult to interpret. Thus, instead of having to consider

19 variables, it was necessary to deal with, on average, no more than five.

2.4 RAINFALL DATA

Rainfall data for this study have been taken from the South African Weather Bureau publication 'Climate of South Africa. Part 10. District Rainfall' (South African Weather Bureau, 1972). The country has been divided by the South African Weather Bureau into a number of homogeneous rainfall districts, each district value being a mean of station rainfalls for a given area. Such values may be accepted as the relevant district rainfall provided that the number of stations is adequate (greater than 5) and that they are fairly evenly distributed. These conditions having been met, a district series then has the advantage of applying a slight smoothing to the data and thus decreasing noise effects.

In this dissertation a coarse grid of 20 district centres



Fig 2.2 Rainfall district centres

has been used (Fig 6.2) to provide monthly totals of rainfall (mm) for which data were available from 1951 to 1975.

Unavoidably, this is two years shorter than the pressure data series.

2.5 STEPWISE MULTIPLE REGRESSION

Many different regression techniques are available to determine the form of a linear relationship between a given dependent variable and a set of possible explanatory variables. Stepwise multiple linear regression was chosen for reasons of economy to describe the relationships between pressure fields derived by principal components analysis and monthly rainfall over the Republic of South Africa. Rainfall, the dependent variable, was regressed on the time series of principle component scores which were taken as the independent variables in the regression.

Ordinary multiple linear regression analysis pulls in all the independent variables offered up to the procedure. Alternatively the stepwise method considers the effect of each variable on the whole regression. It therefore provides information about the order of importance of the individual independent variables in relation to the dependent variable, given that the previous independent variables are already in the regression. Forward selection (Chatterjee & Price, 1977) was used to insert variables into the regression

equation. This process is terminated when the partial F -value at some convenient level of significance becomes statistically insignificant for the most recently returned variable. The order in which variables are included depends on the partial correlation coefficients. These are a relative measure of the importance of the variables, not yet entered into the regression equation, ability to account for the dependent variable's variance. In the present case an F -to-enter of 10% was used (Draper and Smith, 1966). At each step, variables already in the equation are re-examined in the light of their interrelationships with the variables entered at a later stage. Any variable thus found to no longer make a significant contribution in explaining the dependent variable's variance are then removed from the regression equation. This feature, therefore, also makes stepwise multiple regression suitable for data matrices with a high degree of collinearity. However, since principle components are uncorrelated, this facility was not utilised in this work.

* * * *

The techniques discussed are well suited to determine the nature and spatial variability of the pressure fields over the oceans surrounding southern Africa and for the study of the relationships between rainfall and the derived pressure fields. In the following chapter the first of the pressure fields defined by the analysis will be considered.

CHAPTER 3

MEAN PRESSURE PATTERNS AND THE GENERAL PRESSURE FIELD

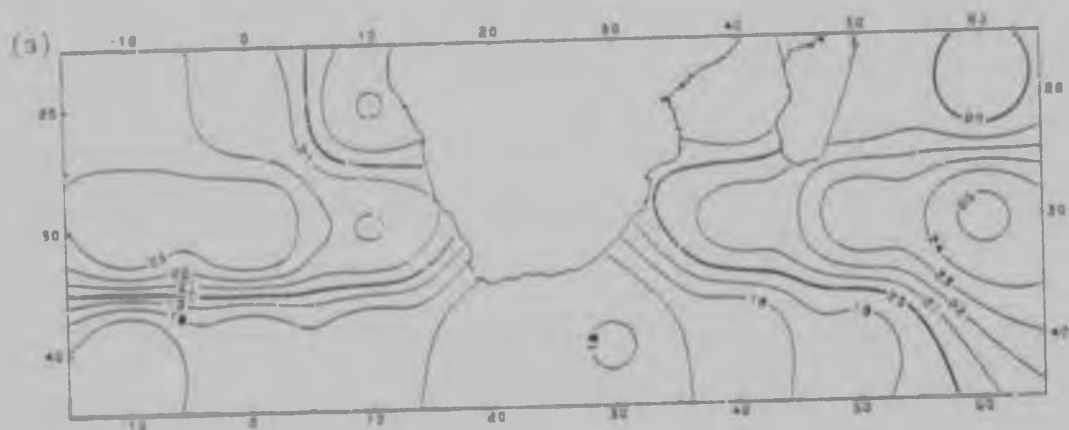
3.1 INTRODUCTION

Whereas it is the departures from mean circulation patterns that produce the weather-forcing mechanisms, it is necessary to define and understand the underlying controls reflected in the mean pattern. Decomposition of the oceanic sea-level pressure data by principal components reveals three major pressure fields. In this chapter the most important of these fields, termed the general pressure field, is discussed.

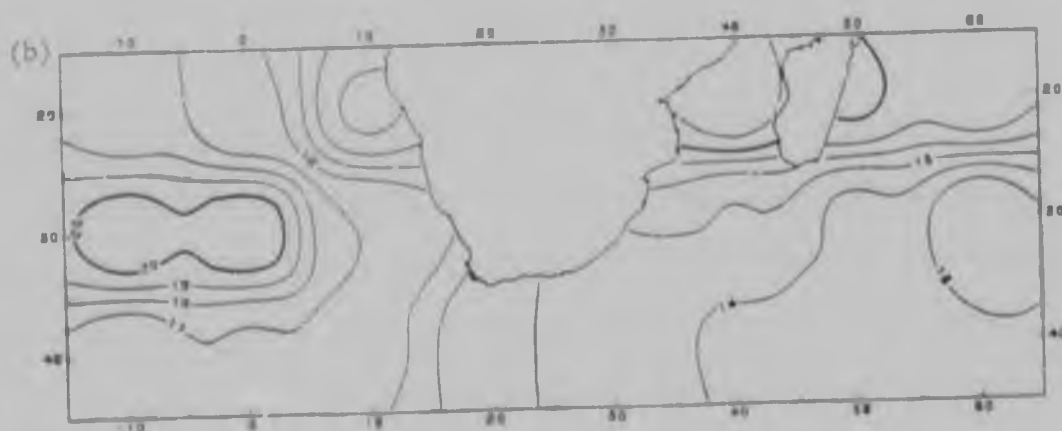
3.2 MEAN MONTHLY PRESSURE PATTERNS

Mean monthly pressure maps have been constructed to show the annual march of sea-level pressure over the oceans surrounding southern Africa. Oceanic sea-level pressure, in general, may be described in terms of two major high pressure centres. The Atlantic Ocean high is situated off the west coast of the subcontinent, the Indian Ocean high off the east coast.

In both summer and winter, the mean circulation is dominated by the high pressure centres. The highest mean pressure value over the Atlantic Ocean (1024 mb) is found in July, while the Indian Ocean maximum (1025 mb) occurs in August [Fig 3.1a]. During these winter months, pressure centres are closest to the subcontinent. Lowest pressures are found over both oceans during February [Fig 3.1b]. A complete monthly set of mean pressure charts is given in Appendix 1.



August



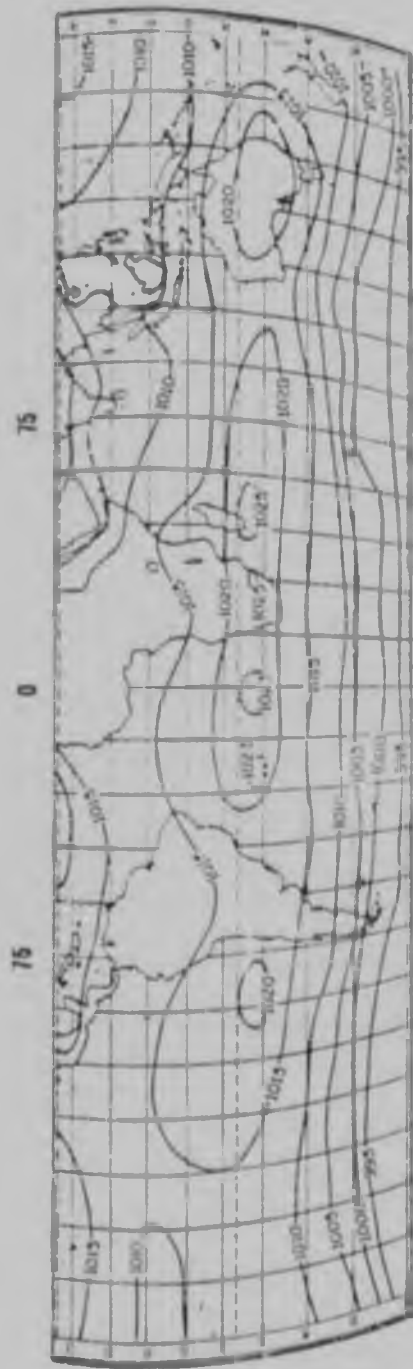
February

Fig 3.1 Mean monthly pressure distributions.

Pressure values are given as mean sea-level pressures +1000 mb i.e., 20 must be read as 1020mb.

Two aspects of the described mean pressure system stand out in these maps. First, a lead-lag relationship exists between the sun's apparent migration in declination and months showing the maximum and minimum pressure situations. The summer solstice occurs on 21st December when the sun reaches its maximum southerly declination; the winter solstice is on the 21st June. Secondly, there is an unequal annual change in intensity and position of the two high pressure centres. The Atlantic Ocean high is relatively stable, exhibiting only a slight shift southwards during the summer months. The range of mean pressure of the centre of this anticyclone varies from 1020 mb to 1024 mb. The centre of the Indian Ocean high on the other hand, suffers a far larger displacement, but to the east, during the summer months and has a wider pressure range of 1015 mb to 1025 mb in the area under consideration. The maximum eastward displacement of this cell is centred at approximately 80° E and is not apparent from the area under consideration (Fig 3.2).

Pressure gradients associated with the mean monthly fields vary across the oceans throughout the year. Gradients appear sharpest around the Atlantic Ocean high, while those around the Indian Ocean high show variation with its approach and departure from the subcontinent. To the south, the Indian Ocean high pressure centre gradients are weak from September through to April, after which contours show a steeper gradient. The situation to the north of the Indian Ocean high shows relatively steep gradients throughout the year.



June



January

Fig 3.2 Mean sea-level pressure distribution (after Critchfield, 1966).

3.3 PRESSURE FIELDS

Principal components analysis has been used to isolate uncorrelated patterns in the monthly oceanic sea-level pressure data. Resulting patterns of sea-level pressure fields have been sorted by the month. Whereas Craddock and Flood (1969) have carried out principal components analysis on a single series constituted by monthly values over a number of years, in this study twelve different series of monthly pressure values from 1951 - 1977 were analysed.

Of the nineteen components derived for each month, only four to six met Kaiser's criterion of greater than unity (greater than one). For each of the four to six significant components, monthly maps of the spatial distribution of eigenvector loadings were determined. These were then sorted, by visual inspection, into three distinctly evident patterns with common characteristics. The three pressure fields are henceforth identified as:

- (i) a general pressure field,
- (ii) an east-west pressure field in which longitudinal contrasts predominate (henceforth called the longitudinal pressure field), and
- (iii) a north-south field showing strong latitudinal contrasts (henceforth called the latitudinal pressure field).

The principal component distribution for each pressure field is given in Table 3.1.

The general pressure field accounts for an average of 33.2 percent of the total variance encountered in the overall pressure field. The longitudinal field accounts for an average of 22.1 percent and the latitudinal for 15.3 percent (Table 3.2). The percentages apply to the year as a whole; they do not necessarily apply in the case of individual months.

Table 3.1 PRINCIPAL COMPONENT DISTRIBUTION (by number)
ACCORDING TO PRESSURE FIELDS.

	GENERAL	LONGITUDINAL	LATITUDINAL	TOTAL VARIANCE
Oct	1	2	3	73.5
Nov	1	3	2	75.3
Dec	1	3	2	66.4
Jan	1	2	3	74.6
Feb	1	3	2	72.9
Mar	2	1	3	67.0
Apr	1	2	3	61.1
May	1	3	2	66.3
Jun	1	2	3	76.4
Jul	1	2	3	69.8
Aug	1	2	3	76.4
Sep	1	2	3	77.1

Table 1 PERCENTAGE VARIANCE ACCOUNTED FOR BY EACH PRES-
SURE FIELD

	NORMAL	LONGITUDINAL	LATITUDINAL	TOTAL (%)
Oct	31.2	—	14.2	75.3
Nov	—	18.2	21.1	66.4
Dec	—	18.1	18.5	74.6
Jan	—	23.7	—	72.9
Feb	—	19.1	25.9	67.0
Mar	—	4	13.1	61.1
Apr	—	—	17	66.3
May	—	17	21.4	76.4
Jun	—	0.8	12.1	69.8
Jul	—	—	17.3	76.4
Aug	—	—	—	77.1
Sep	—	—	8.7	71.4

3.1.1. Distribution of eigenvectors

The distribution of eigenvectors for the general pressure field contain mostly positive loadings with high values over both oceans. October through March show high loadings over the Atlantic Ocean, whereas May to August, with the exception of June, have large values over the Indian Ocean. Both oceans are equally emphasised during April and September.

Most grid points have positive eigenvector loadings for the general pressure field (Fig 3.3). The loadings are correlation coefficients between the components and the original pressure data and hence, high values for a grid point indicate that it is well represented by the general pressure field (and vice versa).

3.5 SEASONAL CHANGES IN GENERAL PRESSURE FIELD

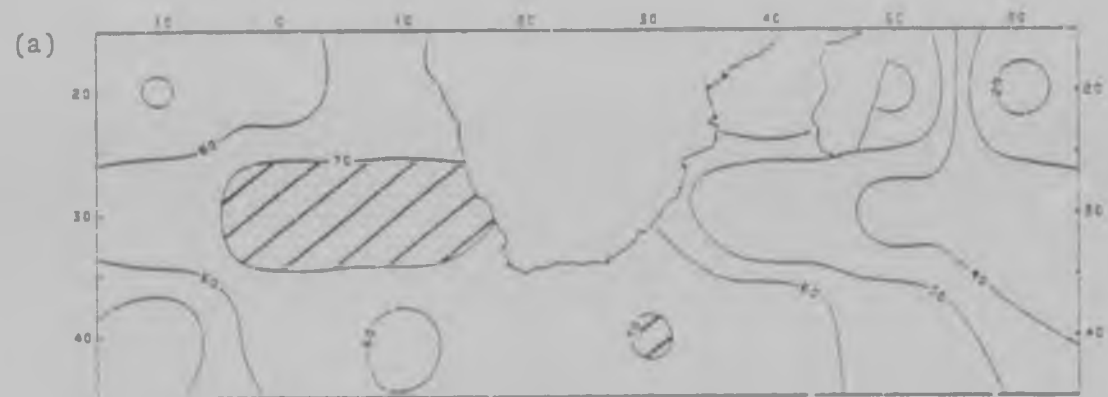
Summer conditions

During the summer period, October to March, certain common characteristics are apparent in the general pressure fields. In October, higher loadings are found to the west, south-west and south of South Africa (Fig 3.4a). By contrast, in the Indian Ocean sector loadings are somewhat lower. However, in general, the relief of the correlation fields is not pronounced. November shows a strengthening of values to the west of the subcontinent (Fig 3.4b), whereas the field over the Indian Ocean shows little relief.

During December the general pressure field begins to strengthen markedly to the south-west of Cape Town (Fig 3.4c). At the same time in the Indian Ocean sector, particularly to the north, the field has weakened. This trend is constant through January to March, particular emphasis being placed on the south-western oceanic areas south of the subcontinent.



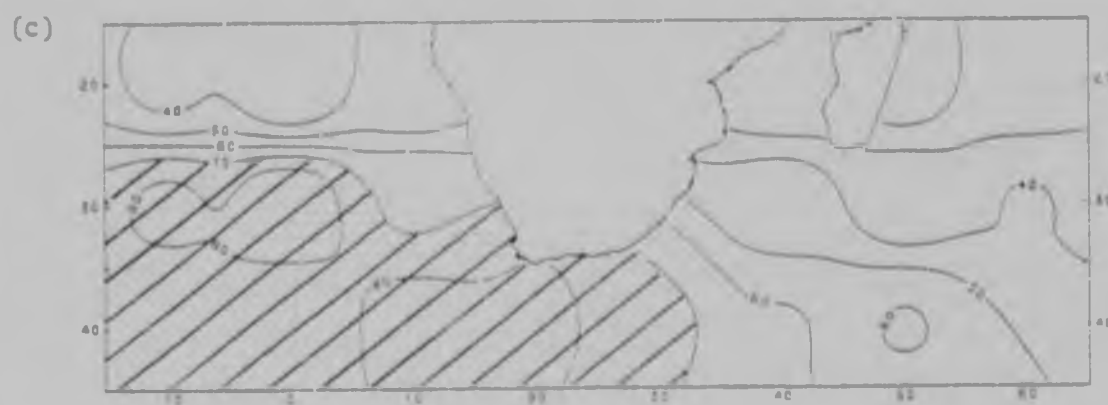
Fig 3.3 Eigenvector loadings, by grid point, for the general pressure field (which is represented by the first principal component for all months except March).



October

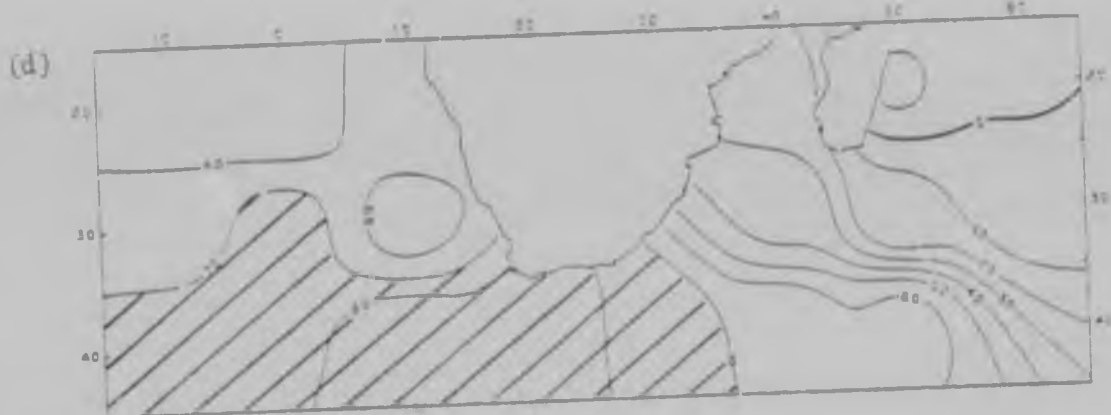


November



December

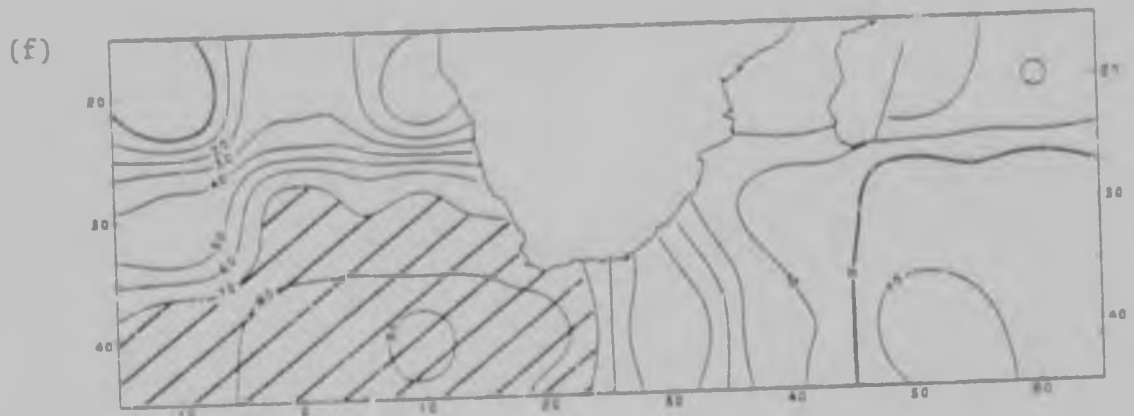
Fig 3.4 General pressure field: summer conditions
(eigenvector loadings x 100)



January



February



March

Fig 3.4(cont.) General pressure field: summer conditions (eigenvector loadings x 100).

The Winter Pattern

Unlike the summer months, May, July and August show high eigenvector loadings over the Indian Ocean. In June the area west of the subcontinent is emphasised.

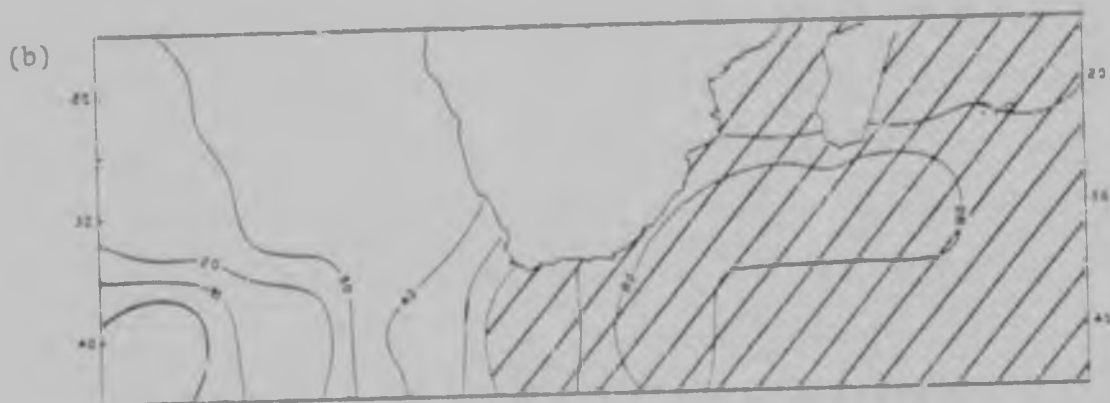
During May, high values are found east of the South African coast (Fig 3.5a). East-west gradients are found over the Atlantic Ocean, but this area is less well represented by the general pressure field. In July high loadings (greater than 0.7, that is, 70 on the maps) are found over the whole Indian Ocean area (Fig 3.5b). The intensity and size of the field decreases somewhat during August (Fig 3.5c). The winter months, May to August, are predominantly characterised by large positive anomalies over the Indian Ocean area (see Appendix 3).

Transition Periods

April and September represent between-season conditions. Both months show equal loadings over both oceans (Fig 3.6). During April, the high values south-west of Cape Town characteristic of the summer months, weaken and the beginning of the winter Indian Ocean predominance in the general pressure field is observed. The reverse takes place in September as the Indian Ocean eigenvector loadings decrease in intensity and spatial coherence and Atlantic Ocean values begin to increase.



May

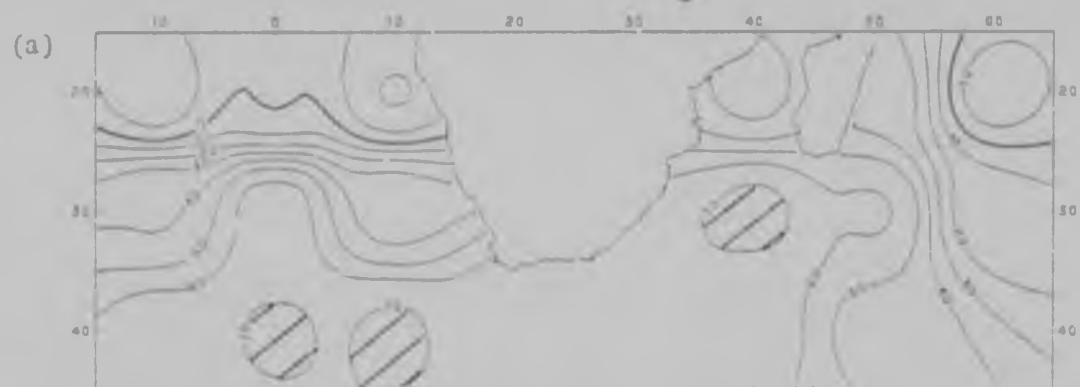


July

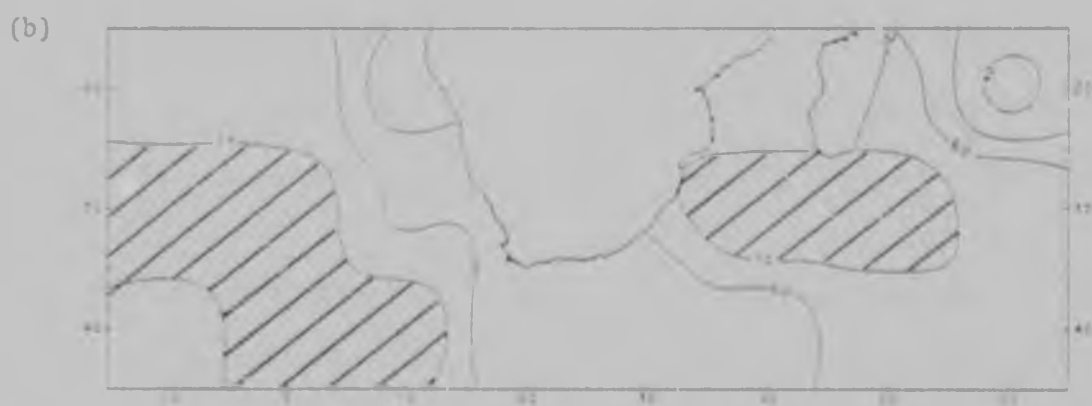


August

Fig 3.5 General pressure field: winter condition
(eigenvector loadings x 100)



April



September

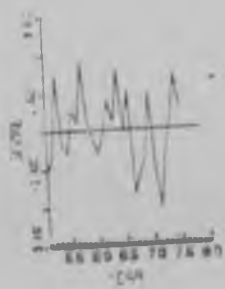
Fig 3.6 General pressure field: transition periods
(eigenvector loadings x 100)

The general pattern that emerges from this discussion of summer conditions is one of developing positive anomalies to the south-west of the subcontinent in the vicinity of longitudes 10° E to 10° W and latitudes 30° S to 44° S.

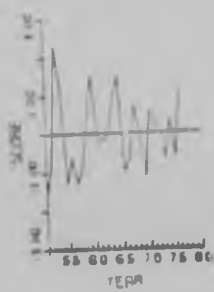
3.6 TEMPORAL VARIATION OF THE GENERAL PRESSURE FIELDS

Monthly principal component scores show little systematic year-to-year variation (Fig 3.7). The series are too short to carry out spectral analyses. Kendall's turning-point test (1973) was used instead to investigate a null-hypothesis of randomness in the series. In no case could the null-hypothesis be rejected at the 5% level, suggesting that the component scores fluctuate in a random manner.

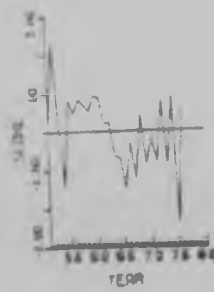
Examples of mean monthly synoptic situations are given for some years with high scores (Fig 3.8). The anomalous pattern for October 1973 represents a summer situation (that is, the eigenvector loadings are representative of pressure deviations from the long-term mean). During 1973, this month achieved a high negative score. The mean monthly synoptic situation for this month compares well (except for sign) with the general pressure field shown in Fig 3.3a, the sign of the eigenvectors being arbitrary (Barry and Perry, 1973). Fig 3.8a illustrates the physical reality of the derived



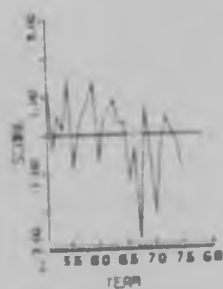
October



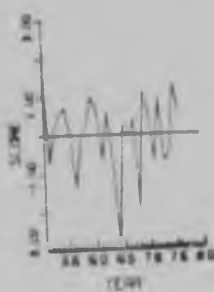
November



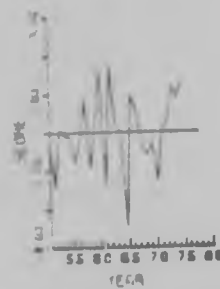
December



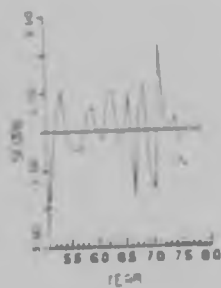
January



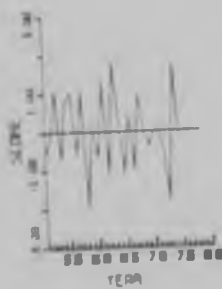
February



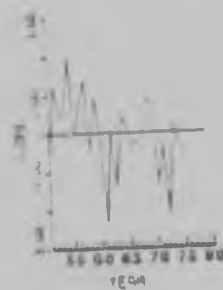
March



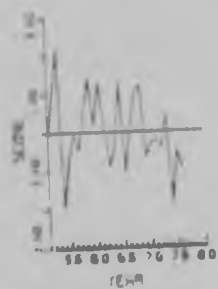
April



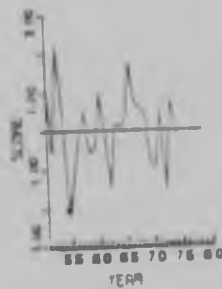
May



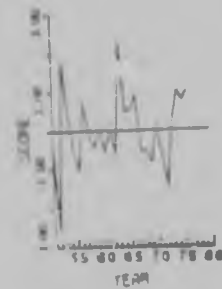
June



July



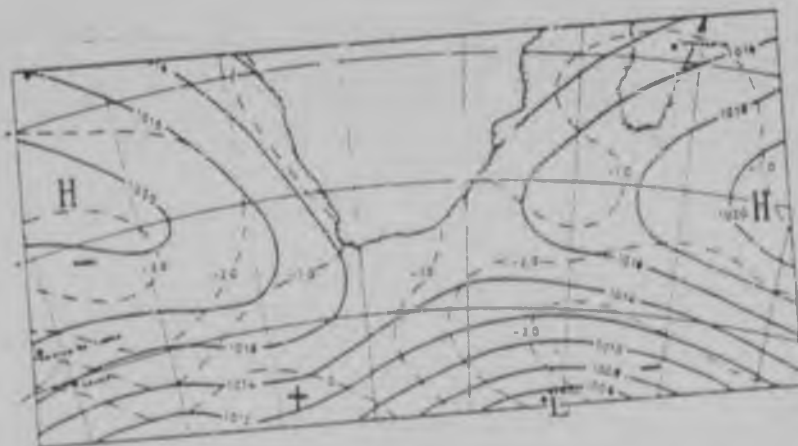
August



September

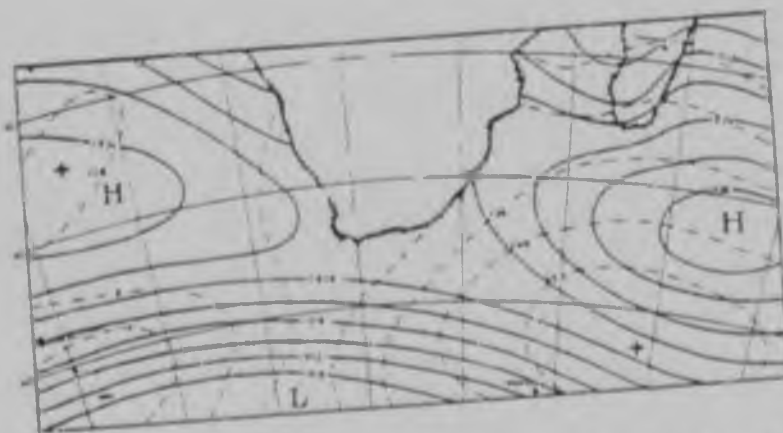
Fig 3.7 Principal component scores for the general pressure field.
(The final score value appears for the year 1976 instead of 1977 and proportionate adjustment should be made in reading the x-axis)

(a)



October 1973: summer conditions with a high negative principal component score.

(b)



August 1967: winter conditions with a high positive principal component score.
mean sea-level isobars (mb)

deviation from 10 year mean (mb)

Fig 3.8 Mean monthly synoptic charts. (S A Weather Bureau).

pressure patterns. In the second instance, quoted in Fig 3.8b, a typical example of a winter situation (August 1967) shows strong positive pressure anomalies over the Indian Ocean sector and illustrates a situation represented by Fig 3.5c.

3.7 DISCUSSION

During the summer high positive loadings in the south Atlantic area to the south-west of Cape Town are prominent features of the general pressure field. By contrast, in winter the mass balance changes and lower values of anomalies appear to be the climatological norm for the southern Atlantic Ocean area south-west of Cape Town. Such changes occur as result of changes in the Atlantic Ocean high and probably can be related to the seasonal variation in the position of the subtropical ridge of the zonal standing wave 1 (Fig 3.9). This peak exhibits a 5° latitudinal shift poleward from summer to winter (van Loon & Jenne, 1972).

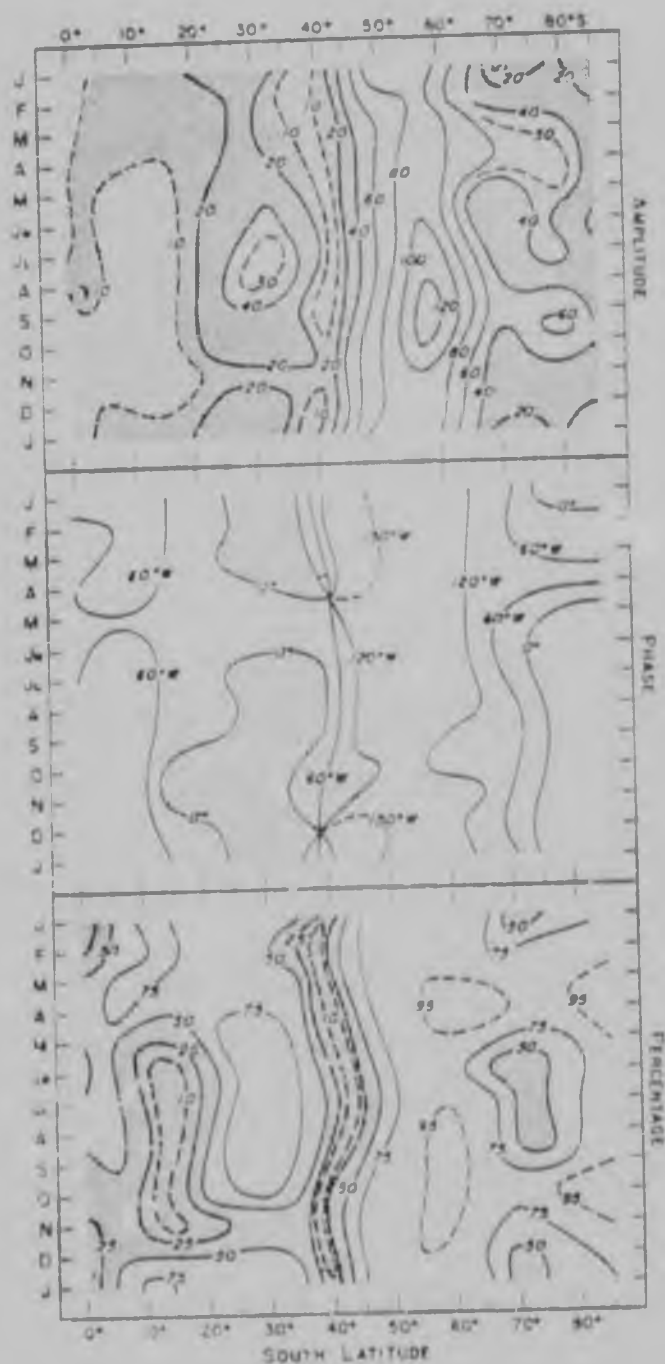


FIG. 5. The annual march of the amplitude (meters) and phase (longitude of ridge, middle) of the standing wave 1 at 500 mb, and of the percentage which it accounts for in the total variance (bottom). (van Loon & Jenne, 1972.)

It has been shown that the general pressure field exhibits distinct seasonal changes that can be related to similar changes in the general circulation of the atmosphere. This feature is characteristic of the Atlantic Ocean to the southwest of Cape Town during the summer period, and of the Indian Ocean during the winter. East-west changes are a feature of the general pressure field to be discussed in the following chapter.

CHAPTER 4

THE LONGITUDINAL PRESSURE FIELD

4.1 INTRODUCTION

The longitudinal pressure field consists of loading patterns from principal components two and three (Table 3.1) and has been identified by similarities in the spatial patterns of the anomaly fields.

Contours constructed from the eigenvector loadings represent the correlation between the relevant principal component and the original sea-level pressure data. Those areas of the fields with large contour values (regardless of sign) are of major interest because they will be the areas most strongly represented by the principal component. Negative values are found in all correlation fields, in contrast to the general pressure field where few non-positive values were encountered. Within the longitudinal pressure field negative anomalies tend to characterise one ocean and positive the other. Eigenvector loadings clearly show this dichotomous trend between the oceans (Fig 4.1). The balance of loading values is seldom equal between the two oceans and two

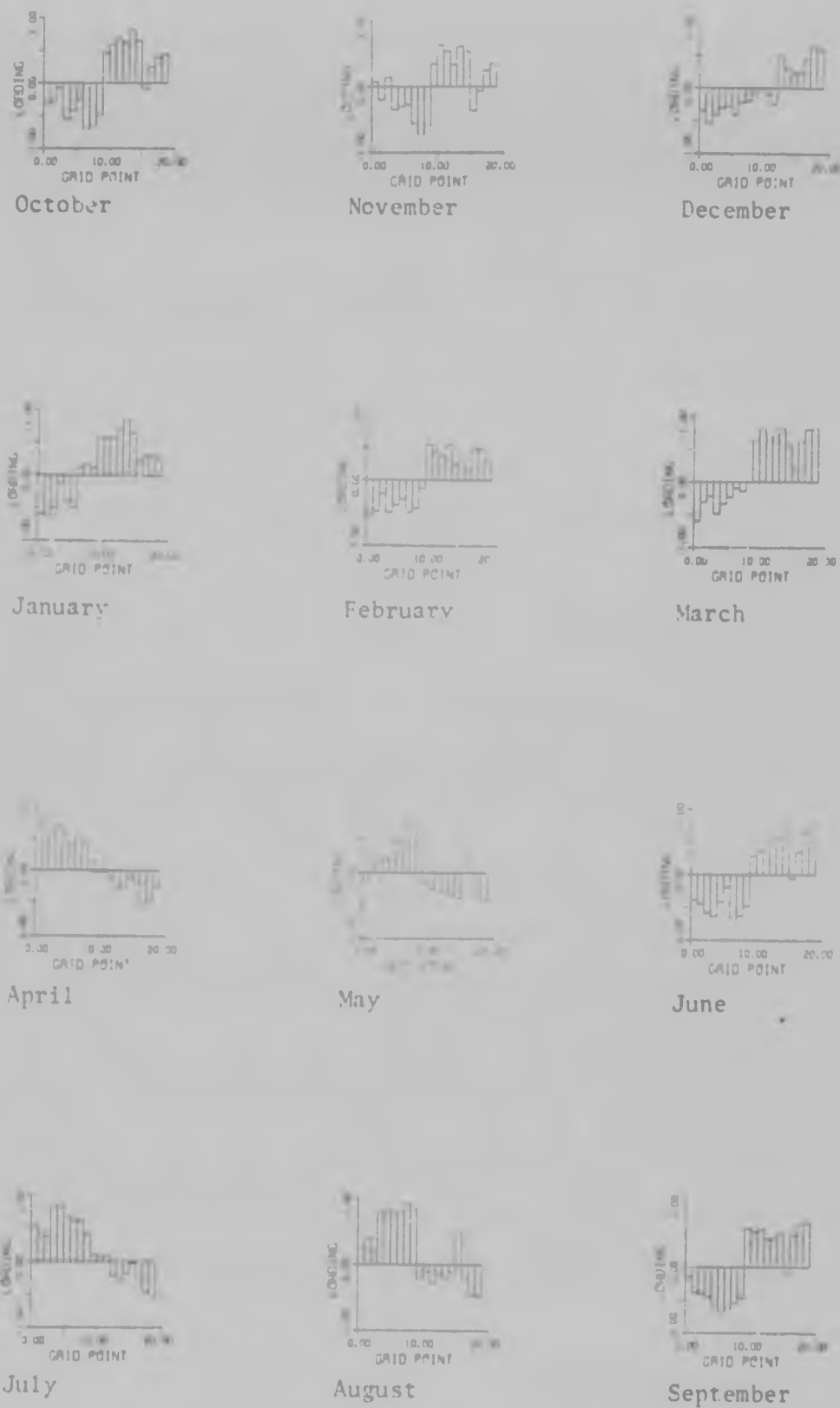


Fig 4.1 Eigenvector loadings, by grid point, of the longitudinal pressure field (being a composite of principal components 2 & 3)

major temporal and spatial patterns may be distinguished: first, that emphasising the Indian Ocean area (October to March); and secondly emphasising the Atlantic Ocean (April to September). The proportion of the total pressure variance accounted for by longitudinal changes in the pressure field is about two-thirds that accounted for by the general pressure field (Table 3.2).

4.2 SEASONAL CHANGES IN THE LONGITUDINAL PRESSURE FIELD.

Summer conditions

During October to March, high loadings occur over the Indian Ocean. Prominent values during October are centered around 30° S 50° E (Fig 4.2a). Anomaly gradients are generally weak for the remainder of the field. January shows a northward extension of the area strongly represented by the longitudinal pressure field (Fig 4.2b). During March, anomaly gradients are again weak, but the whole Indian Ocean sector has loading values greater than 0.6 (that is, 60 on Fig 4.2c). The other months, November, December and February all show Indian Ocean dominance in loading values (see Appendix 4).

The Winter Pattern

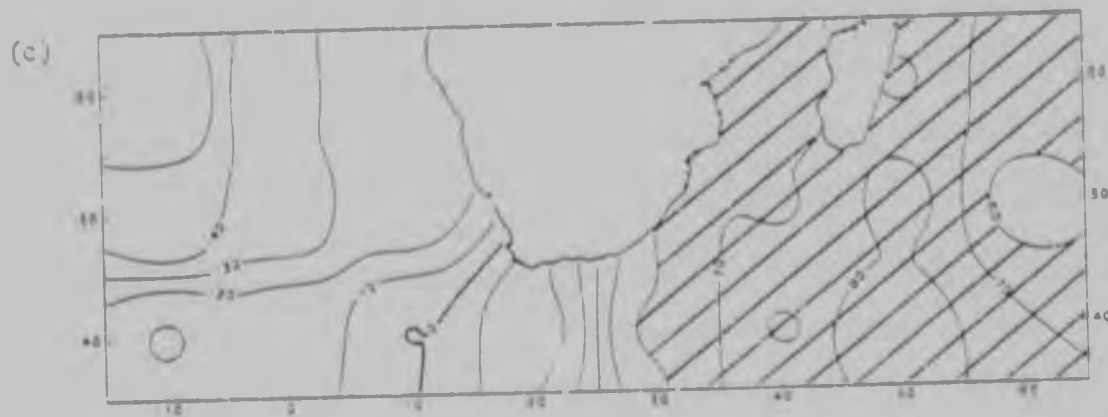
The longitudinal pressure field emphasises the Atlantic Ocean region to the west and south-west of South Africa,



October



January



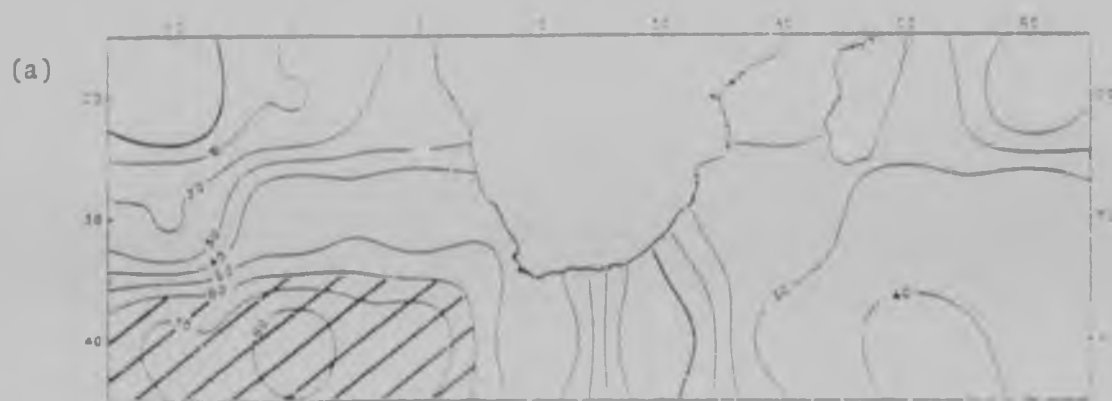
March

Fig 4.2 Longitudinal pressure field: summer conditions
(eigenvector loadings x 100)

encompassing the area south of 25° S and west of 15° E. During May, strong positive anomalies occur south-west of Cape Town (Fig 4.3a). Anomaly gradients weaken markedly towards the Indian Ocean sector. July shows the maximum northward expansion of high loading values (Fig 4.3b). The greatest eigenvector loading values are encountered in the area 35° S and 0° during August (Fig 4.3c). Marked positive anomaly gradients characterise this month.

4.3 TEMPORAL VARIATION OF THE LONGITUDINAL PRESSURE FIELDS

The longitudinal pressure field was not characterised by high scores for similar years from month to month. The most persistently high scores occurred in April to July, 1973, and in January to April, 1974 (Fig 4.4). The mean monthly synoptic chart for January 1961 provides an example of actual summer anomaly conditions for a year of high score (Fig 4.5a). This chart shows a positive - negative anomaly pattern indicated for January for the longitudinal pressure field (Fig 4.2b). The winter deviation pattern is well illustrated by the synoptic chart for May 1973 (Fig 4.5b) which shows anomaly patterns close to those found in the longitudinal pressure field for May (Fig 4.3a).



May

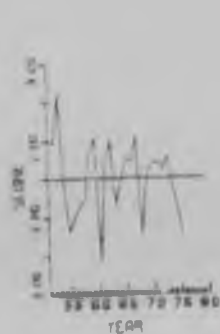


July

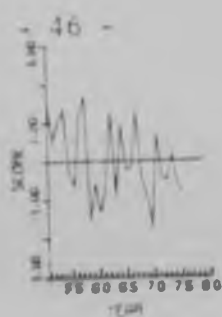


August

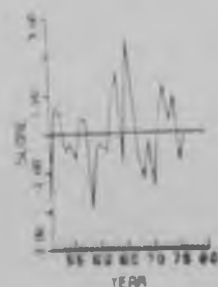
Fig 4.3 Longitudinal pressure field: winter pattern
(eigenvector loadings x 100)



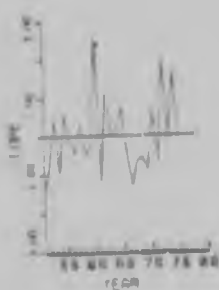
October



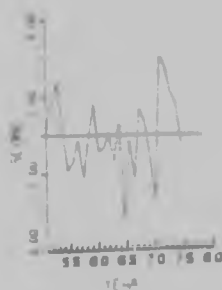
November



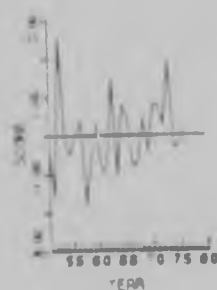
December



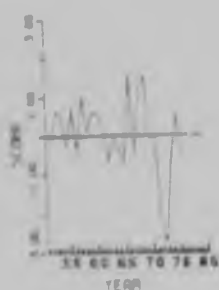
January



February



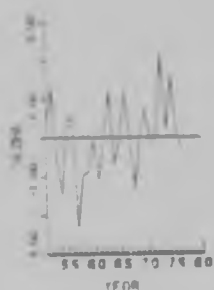
March



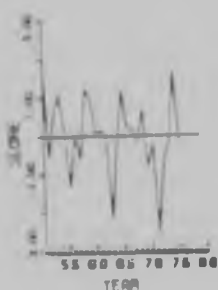
April



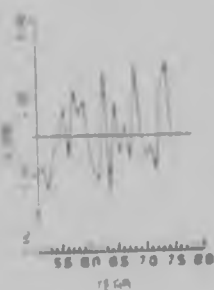
May



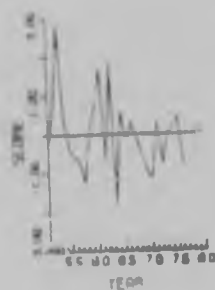
June



July



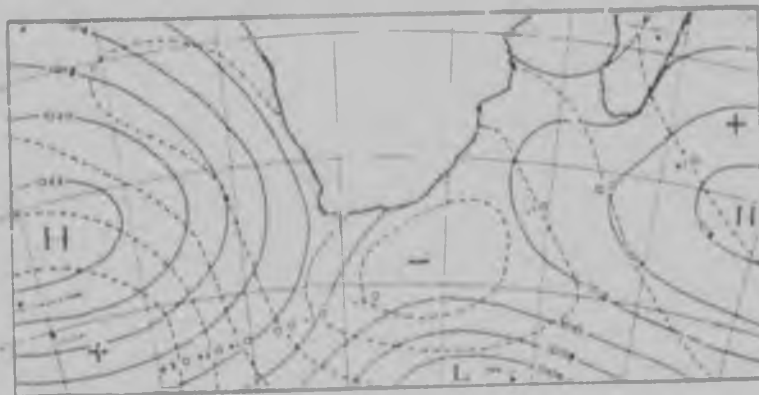
August



September

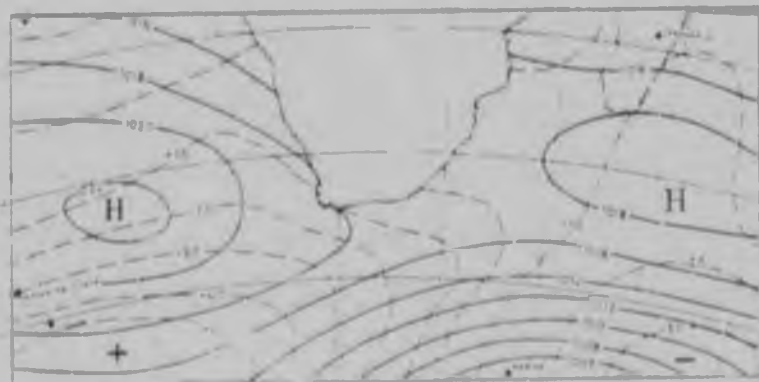
Fig 4.4 Principal component scores for the longitudinal pressure field.

(a)



January 1961: summer conditions

(b)



May 1973: winter pattern

————— mean sea-level isobars (mb)
 - - - - - deviation from 10 year mean (mb)

Fig 4.5 Mean monthly synoptic charts (S A Weather Bureau).

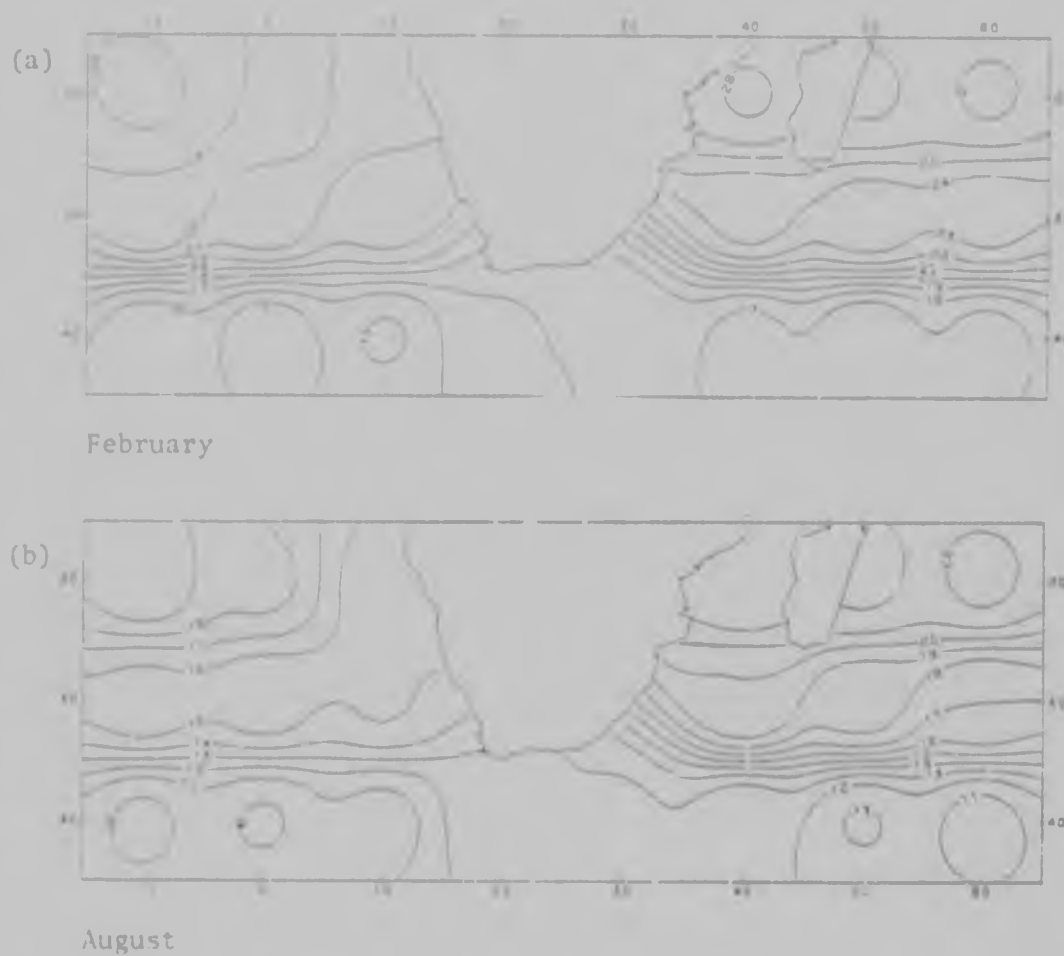
4.4 DISCUSSION

The longitudinal pressure field shows a difference in sign between east and west. Although different oceanic sectors are emphasised during summer and winter periods, weaker anomalies of opposite sign characterise the other parts of the pressure field.

The nature of the teleconnection between the Atlantic and Indian Oceans adjacent to southern Africa immediately brings to mind the 'Southern Oscillation', which is the fluctuation of pressure between the Indian and Pacific Oceans as first noted by Walker (1923, 1924, 1928) and Walker and Bliss (1930, 1932). Many explanations for this observed phenomenon have been put forward. Berlage and Boer (1959, 1960) considered it a standing wave in the atmosphere. Schell (1956) attributed its existence to the difference between temperature of the cool south-east Pacific and the relatively warm Pacific-Indian Ocean region, a mechanism also proposed by Wright (1975).

It is possible that the observed teleconnection might be a feature of the temperature discontinuity between the cooler Atlantic Ocean and the warmer Indian Ocean. Mean sea surface temperature fields were produced from monthly mean temperatures presented in the 'Climate of the Upper Air - Part I - Southern Hemisphere' (Taliaard, *et al.*, 1969)

Both during summer and winter, the Indian Ocean is markedly warmer than the Atlantic (Fig 4.6). A full set of monthly charts is presented in Appendix 2.



data from 'Climate of the Upper Air - Part I - Southern Hemisphere (Taljaard et al, 1969)).

Fig 4.6 Mean sea surface temperature fields, °C.

During the summer months, October to March, strong anomalies are found over the Indian Ocean sector. By contrast, the south-west Atlantic Ocean shows strong loadings during the winter months of April to September. Standing zonal wave 1 exhibits a 5° longitudinal shift between summer and winter

(van Loon & Jenne, 1972), it is possible that the longitudinal pressure field represents standing zonal wave 1 during its winter displacement.

The longitudinal pressure field shows an east-west division of pressure anomalies (as evidenced by the \bar{p} value). The apparent dichotomy has been linked to the temperature difference noticeable between the two oceans adjacent to the subcontinent and is emphasized for the summer months. Winter conditions re-emphasize the importance of standing zonal wave 1 in the oceanic sea-level circulation. In contrast to the east-west division of loadings, a north-south trend is found in the longitudinal pressure field (see also the discussion in the following chapter).

CHAPTER 5

THE LATITUDINAL PRESSURE FIELD

5.1 INTRODUCTION

The latitudinal pressure field in which north-south contrasts predominate is represented by the third principal component for two-thirds of the year and by the second for the remainder of the year. As in the case of the longitudinal pressure field, strong regional changes are apparent throughout the year. Whereas the previously discussed longitudinal pressure field showed contrasts between the Atlantic and Indian Oceans, latitudinal gradients characterise the latitudinal pressure field. The eigenvector loadings for the latitudinal are presented in Fig 5.1.

The latitudinal pressure field exhibits two characteristic features: one characterised by high eigenvector loading values over the northern oceanic areas (December to May); the other by high values in the southern parts of the oceans (June to November). Whereas the two previous pressure fields showed initiation of patterns in October, the latitudinal field shows important changes in December and June. Charts for all months are given in Appendix 5.

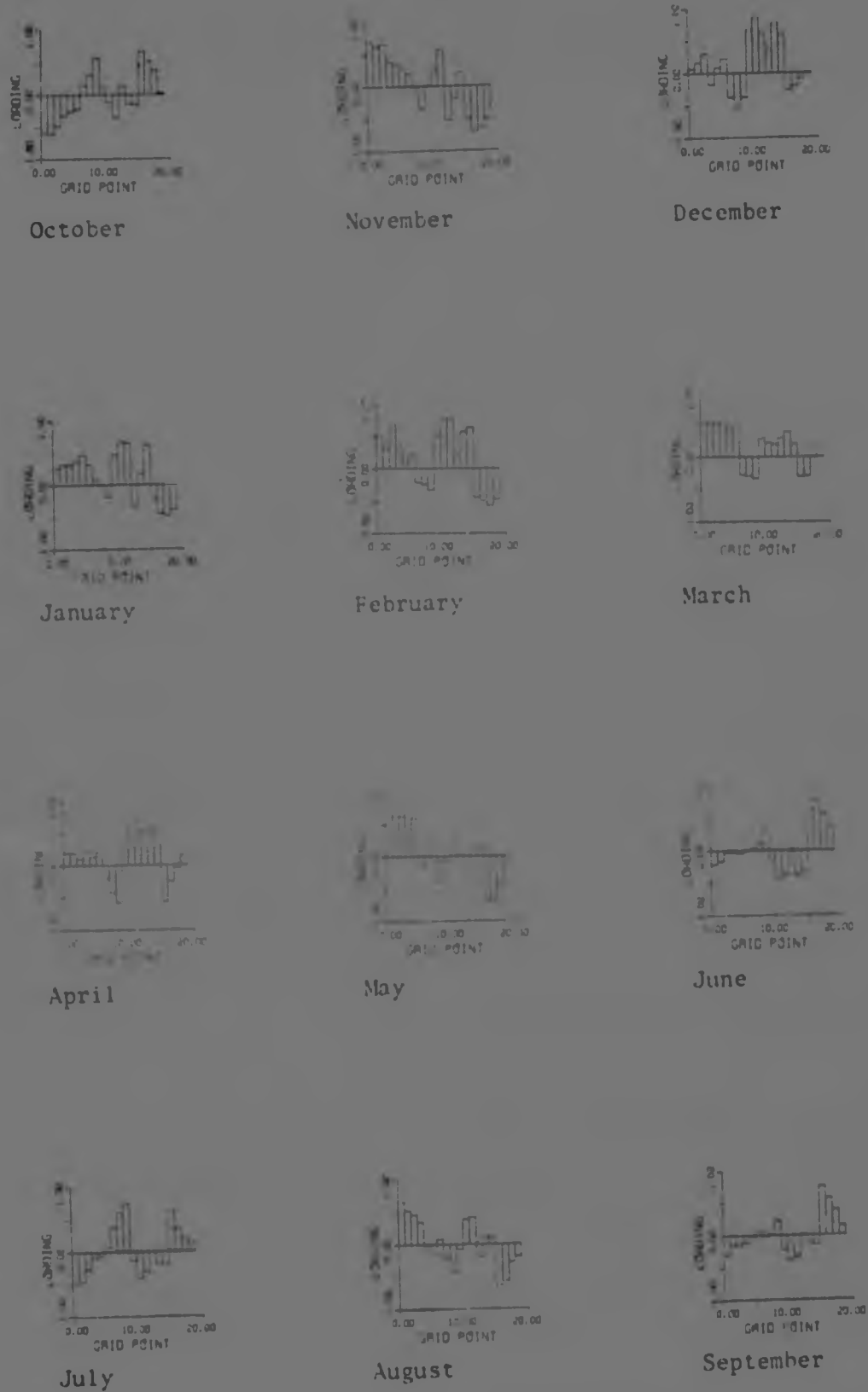


Fig 5.1 Eigenvector loadings, by grid point, for the latitudinal pressure field (being a composite of principal components 3 and 2)

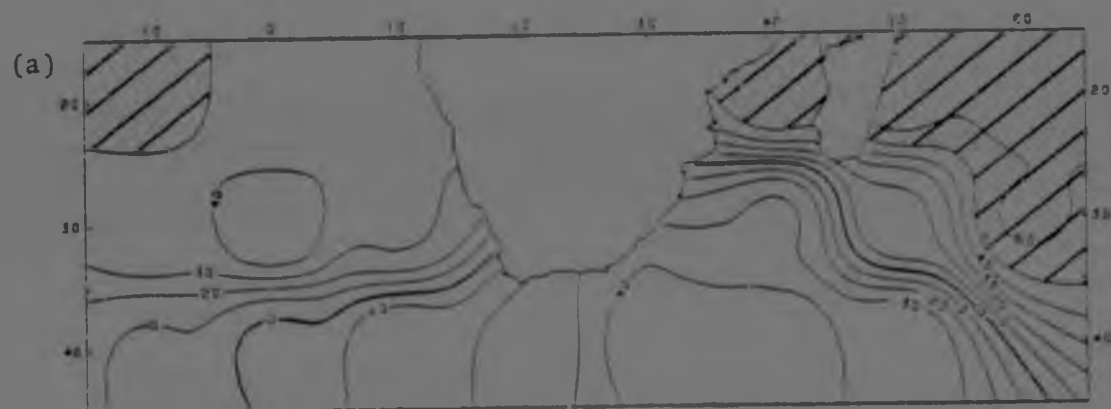
5.2 SEASONAL CHANGES IN THE ZONAL PRESSURE FIELD

Late summer conditions

During December to May highest loadings are found in the northern sections of both the Indian and Atlantic Oceans. The northern area of the Indian Ocean is best represented by the latitudinal pressure field for both January and February (Fig 5.2a & b). During these months, the northern areas of the Atlantic Ocean gain in importance. By March these areas are dominant (Fig 5.2c).

Late winter conditions

The latitudinal pressure field is strongly represented in the Atlantic Ocean area south-west of Cape Town (Fig 5.3). In July an area of high loadings is found at 33° S and between 5° W and 25° E, due south of the subcontinent. During September, the area contracts, shifting to 15° E to 35° E without any latitudinal change, that is, the main anomaly pattern is still south of the subcontinent. Spreading is again evident in October. Strong anomaly gradients are often associated with the Atlantic Ocean.



January

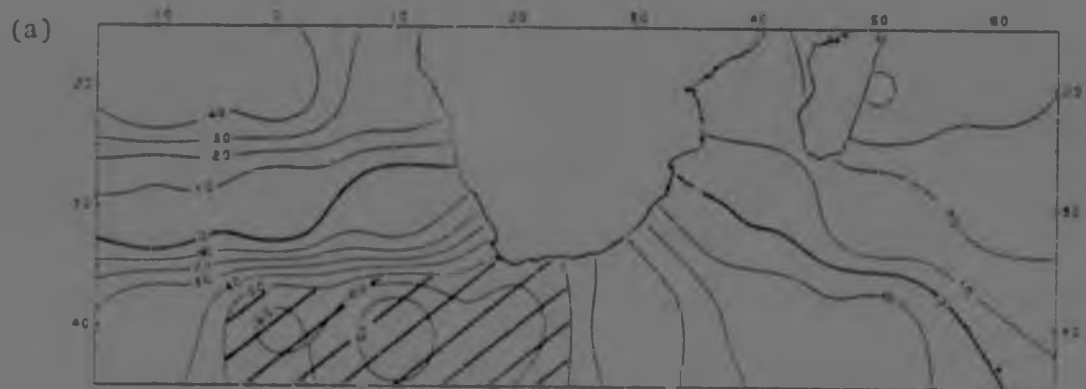


February



March

Fig 5.2 Latitudinal pressure field: summer conditions
(eigenvector loadings x 100).



July



September



October

Fig 5.3 Latitudinal pressure field: winter pattern (eigenvector loadings x 100).

5.3 TEMPORAL VARIATION OF THE LATITUDINAL PRESSURE FIELDS

Each month produces high principal component scores on some years (Fig 5.4). However the years emphasised varied from month to month. The year 1953 consistently produced high scores from January to May, 1970 also showed a persistent tendency during August to November. February 1971 showed a high negative score which is reflected in the strong positive anomaly south, and a negative anomaly to the east of the subcontinent on the mean monthly synoptic chart (Fig 5.5a): An anomaly chart, based on 27 year means, shows the same characteristics (Fig 5.5b).

5.4 DISCUSSION

The latitudinal pressure field shows pronounced north-south gradients throughout the year. The area of strongest pressure anomalies is found to the south, and to a lesser extent, to the south-west of Cape Town. The latitudinal pressure field is linked to the northward displacement of the circumpolar westerlies during winter and the development of a standing trough of low pressure to the south of southern Africa. During summer, the maximum zonal westerlies are situated at 45° S in the Atlantic and Indian Oceanic sectors of the southern hemisphere. The middle latitude zone is also characterised by frequent cyclogenesis (Taljaard, 1967).

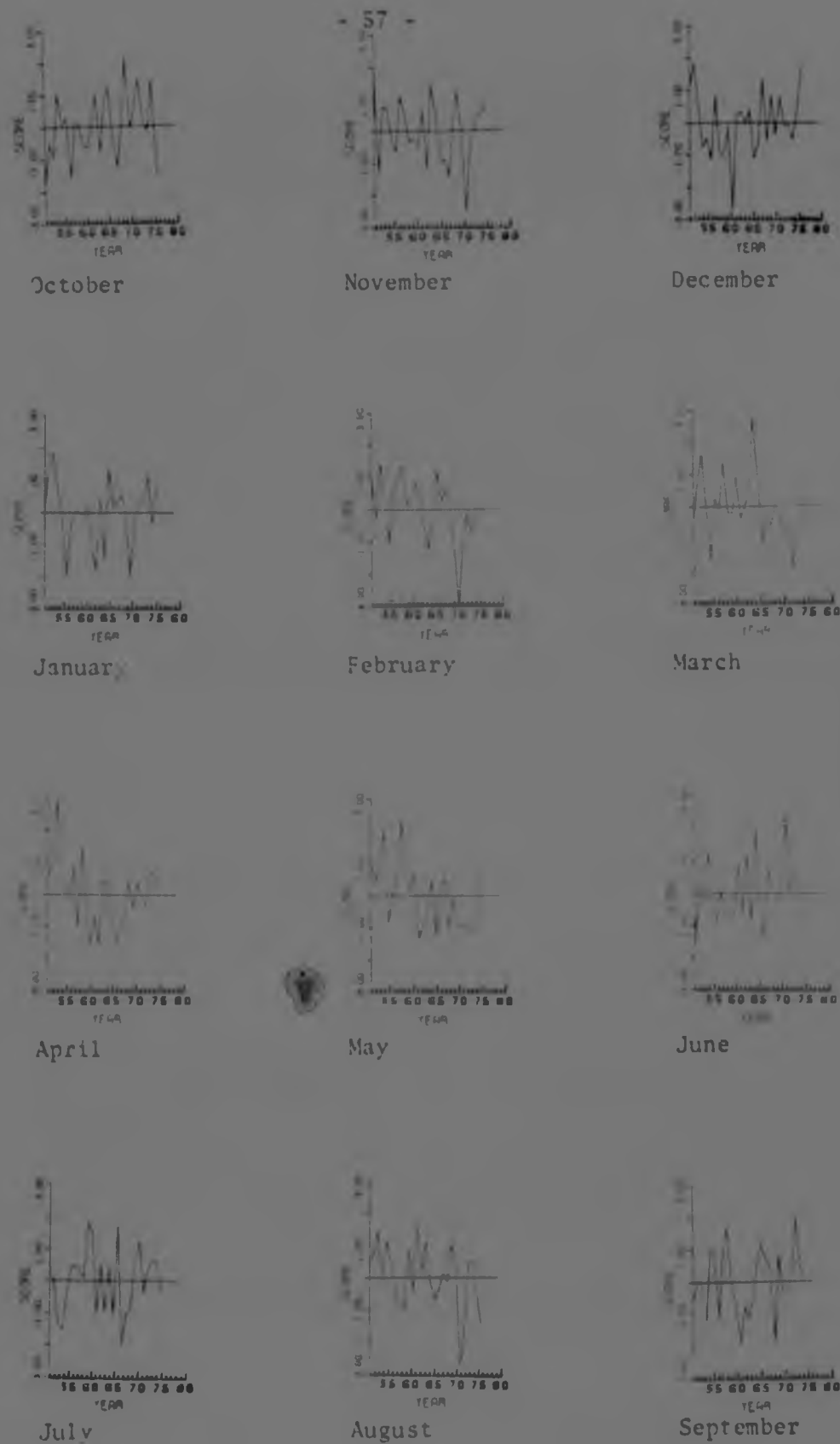
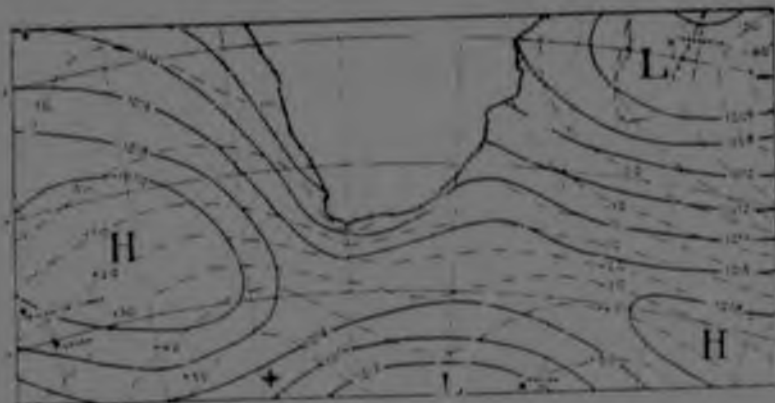


Fig 5.4 Principal component scores for the latitudinal pressure field.

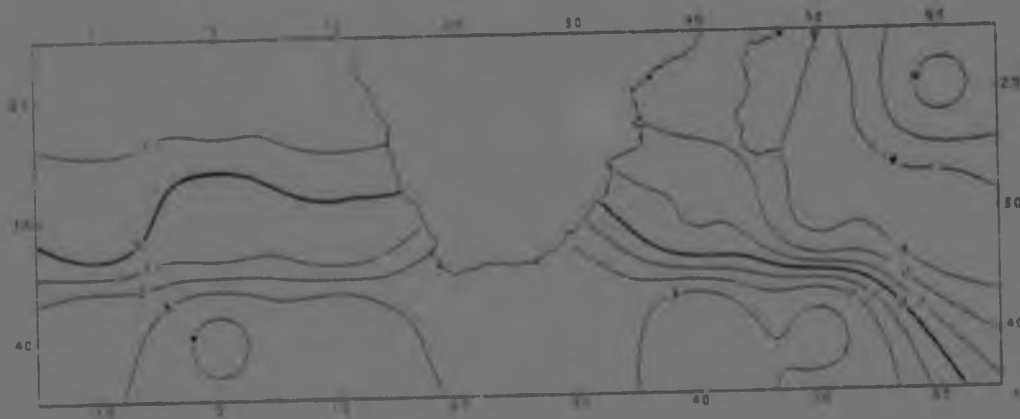
(a)



February 1971 (S A Weather Bureau).

————— mean sea-level isobars (mb)
 - - - - - deviations from 10 year monthly means (mb)

(b)



February 1971

————— pressure deviations from 27 year monthly means (mb)

Fig 5.5 Mean monthly synoptic chart and deviation chart for February 1971.

It is therefore probable that the zonal pressure field represents the movement of the westerly wind belt. During the summer months the poleward movement of the belt results in pressure anomalies in the northern sections becoming important, whereas during the late winter months the northward movement of this belt is emphasised.

* * * *

The latitudinal pressure field exhibits loading values of opposite sign over the northern and southern portions of the oceanic area under consideration. The high anomaly values south of Cape Town during the winter months suggests a winter northward extension of the circumpolar westerlies south and south-west of the subcontinent. Relationships between rainfall and the three pressure fields that have been identified are discussed in the following chapter.

CHAPTER 6

RELATIONSHIPS BETWEEN OCEANIC SEA-LEVEL PRESSURE AND RAINFALL

6.1 INTRODUCTION

Synoptic situations producing daily rainfall are well understood for South Africa. However, long term causal relationships are more difficult to determine. In this chapter an attempt will be made to compare the effects of the oceanic sea-level pressure situations with rainfall over the Republic on a month to month basis.

6.2 ANNUAL MARCH OF RAINFALL OVER SOUTH AFRICA

Using a broad classificatory system, four basic rainfall patterns may be distinguished over the Republic of South Africa (Griffiths, 1972). Fig 6.1 shows the annual pattern of rainfall for representative stations.

Cape Town represents the south-west area of the continent which is characterized by winter maximum rainfall. George shows the characteristic pattern of the area between the winter

maximum in the south-west and south-east. This belt has a double maximum found in the spring (October) and early autumn (March). A distinct summer maximum is experienced over the rest of the Republic, with the greatest amount of rain falling, on average, in the summer months of December to February. A similar belt of summer maximum rainfall may be traced from the southern Cape to Windhoek. In this area, however, the winters are particularly dry and maximum rainfall is found in the month of March. Thus assuming a hydrological year beginning in October, the eastern parts of the country receive rainfall first, that is, in December to February. Maxima also occur in the south-east during this period (usually in October and again in March). Next is an area with a single March maximum stretching northwards between George and Windhoek.

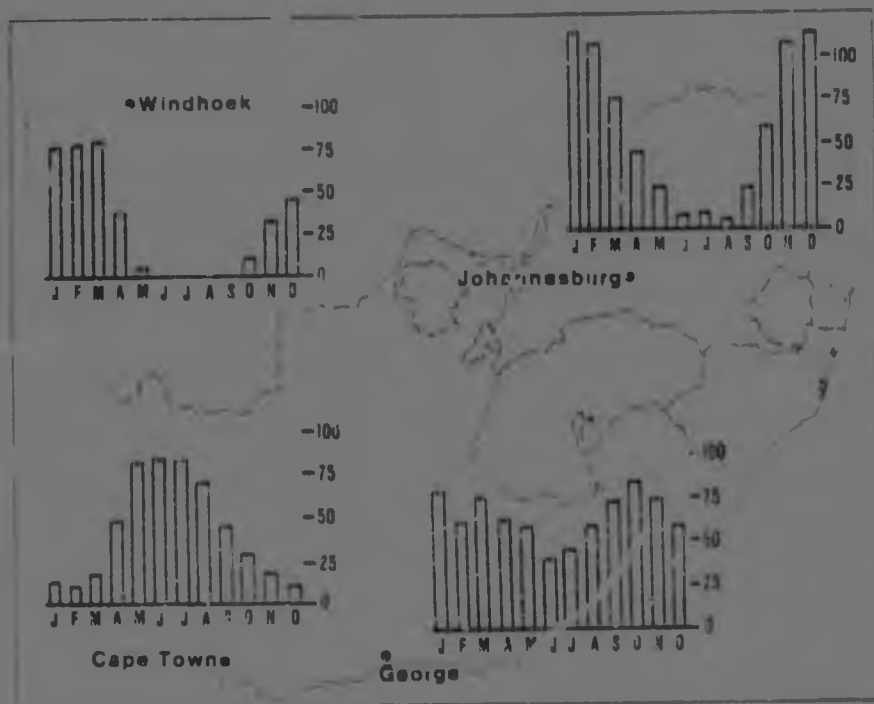


Fig 6.1 Characteristic rainfall patterns over southern Africa (after Griffiths, 1972).

The south-west Cape is the most arid to receive rainfall, having winter maxima towards the end of the hydrological year.

5.3 THE REGRESSION ANALYSIS

Monthly rainfall data have been regressed on the time series of principal components scores. The regression analysis for each month and rainfall district was carried out in two parts: first with a low restriction and secondly with a high restriction criterion.

Low Restriction Analysis

In this analysis the restriction criterion ($F < 0,01$) was applied for the determination of variables into the regression.

Essentially, nearly all the variables (principal components of pressure) were pulled into the regression equation and values of the relative contribution of all these were calculated. For every rainfall district, the principal component resulted in a change in the coefficient of determination as it entered into the regression. The increase in R^2 accounted for by each independent variable was then plotted, per component, against the rainfall district with which it was associated.

Rainfall relationships with the general pressure field.

High coefficients of determination ($R^2 > 20$) exist between rainfall over the continent and the general pressure field. During the summer months, for example November, strong interrelationships exist over the northern parts of South Africa (Fig 6.2a). From November to April a gradual shift takes place (Fig 6.2b). The general pressure field during the winter months is related to rainfall over the south-west Cape (Fig 6.2c). With low loadings for the general pressure field to the south-west of the Cape, in the area where zonal standing wave 1 expresses itself, rainfall over the south-west Cape is enhanced.

Rainfall relationships with the longitudinal pressure field.

Correlations between the time series scores of the principal components analysis for the longitudinal pressure field and rainfall over the Republic, show the highest coefficients of determination (R^2) in the region of the central Cape in January (Fig 6.3a). Since at this time of year it is the Indian Ocean sector of the longitudinal pressure field that is predominant, it appears logical to infer that it is pressure changes in this sector that are of greatest importance in determining rainfall over the central Cape. By contrast, during a typical winter month (Fig 6.3b), the correlation field is flat.



November

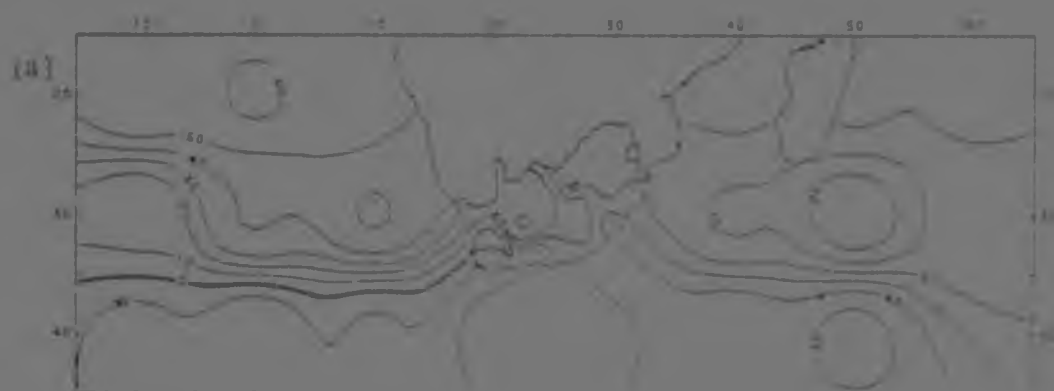


April



July

Fig 6.2 Coefficients of determination (R^2), as a percentage, between rainfall and the general pressure field (mb * 1000).



January



July

Fig 6.3 Coefficients of determination (R^2), as a percentage, between rainfall and the longitudinal pressure field (mb + 1000).

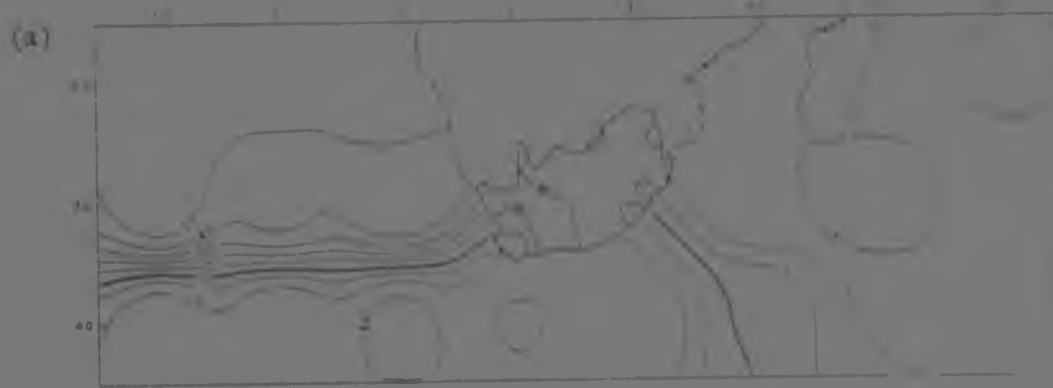
Rainfall relationships with the latitudinal pressure field.

On the whole, the latitudinal pressure field does not account for much of the variance encountered in the rainfall patterns over the subcontinent. There is some suggestion that during the late summer the field is most strongly associated with rainfall over the south-west Cape (Fig 6.4a). By contrast, the winter months, March to October show a relationship between the zonal pressure field and rainfall over the south-western and central parts of the Cape. During the winter, the westerly wind belt exhibits a northerly displacement over the area under discussion. As expected rainfall over the south-west of South Africa (the winter rainfall region) is sensitive to anomalous situations in the westerly wind belt south of the subcontinent.

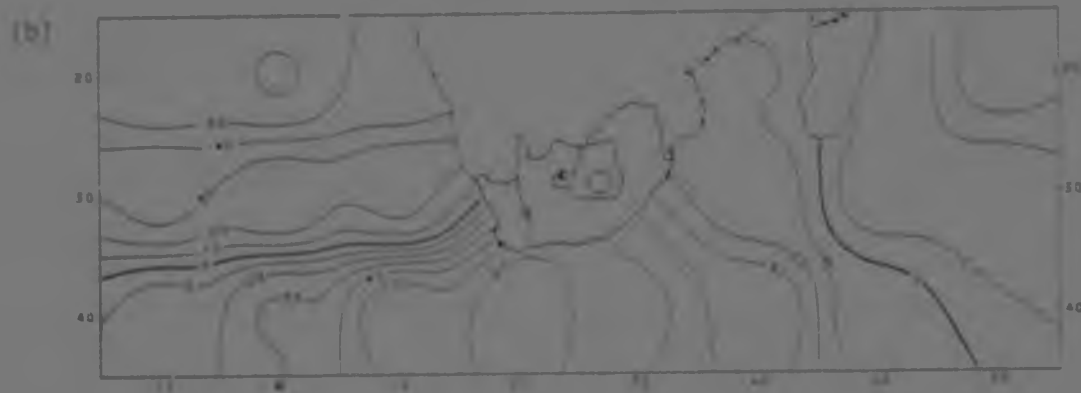
None of the three of the pressure fields described shows strong correlation patterns with rainfall, but each gives some indication of the relationship between the pressure field over the ocean and the transport of moisture of the subcontinent. However, in no way is this indicative of the process operating to produce rainfall.

High restriction regression analysis

Using a higher level of restriction, that is 10 percent level of significance, to govern the entry of variables into the regression analysis, a different set of correlation maps



March (late summer)



October (late winter)

Fig 6.4 Coefficients of determination (R^2), as a percentage, between rainfall and the latitudinal pressure field (mb + 1000).

may be derived to link pressure changes over the oceanic areas to rainfall over the subcontinent. In preparing these maps, the combined coefficient of determination (R^2) of all nineteen principal components derived in the original study, was determined for each rainfall district and contour maps for each individual month prepared therefrom (Fig 6.5). The resulting fields showing the spatial distribution of R^2 indicate the combined effect of the linear relationship between rainfall and the various pressure fields taken together and not individually as in the previous low restriction analysis. Regression equations for individual stations are given for each month (Appendix 6). Tables indicating the pressure components that were pulled into the regression equation at the 10% level of significance for each station, are presented in Appendix 7. Few variables entered persistently and systematically into the equation.

From October to January, the area of maximum correlation between the pressure fields and rainfall over South Africa migrates from the east coast (Fig 6.5a) to the west coast (Fig 6.5d). Whereas October shows two small areas of high correlation on the east coast, November shows a northward and eastward spread (Fig 6.5b). During December, the central Cape area is included with the area of high correlation in the east (Fig 6.5c). January and February represent maximum summer conditions (Fig 6.5d & c).



Fig 6.5 High restriction coefficient of determination, by month, between rainfall and the combined principal components.

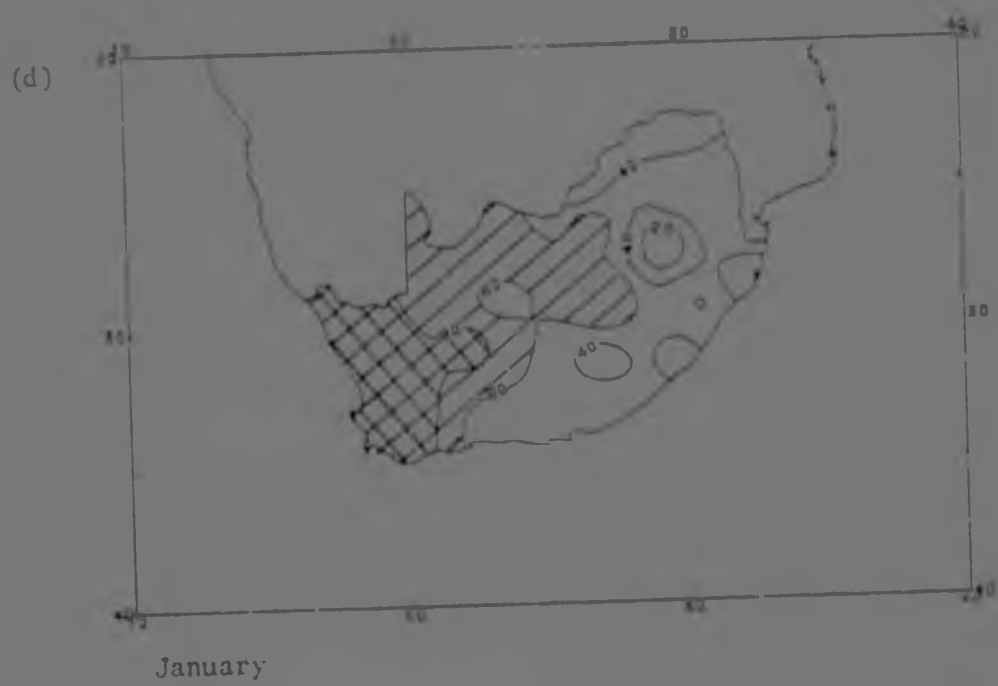
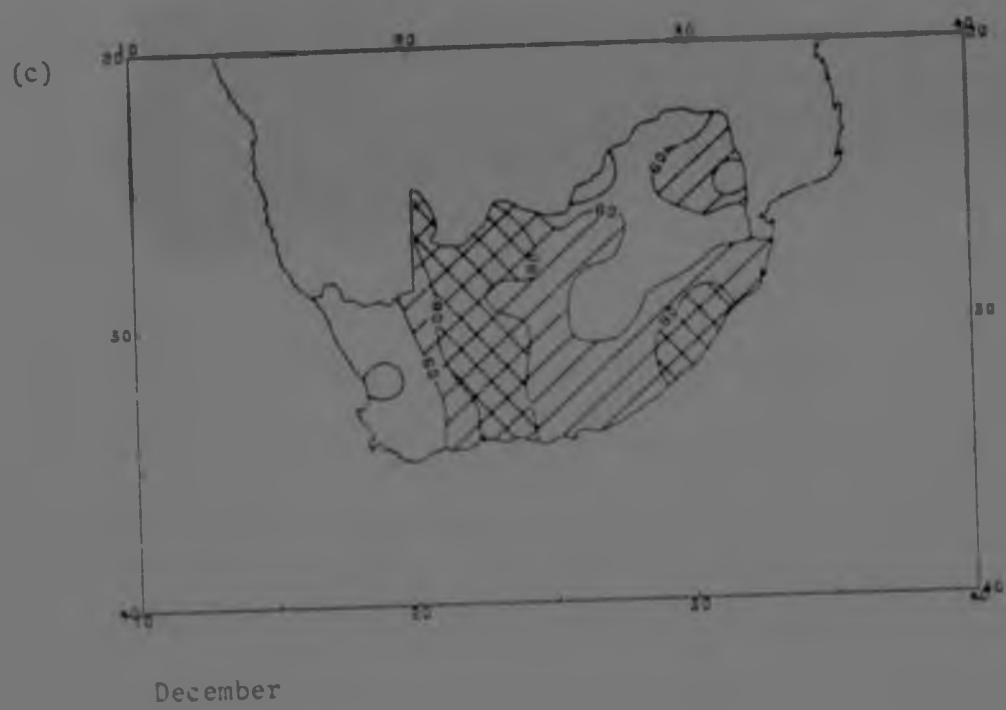


Fig 6.5 (Continued)

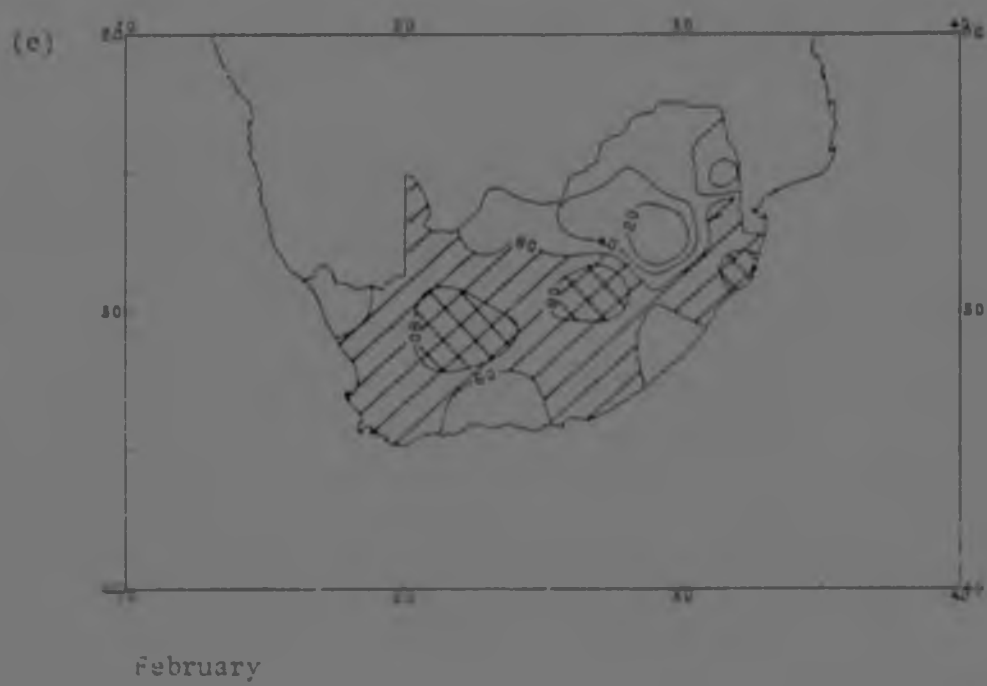
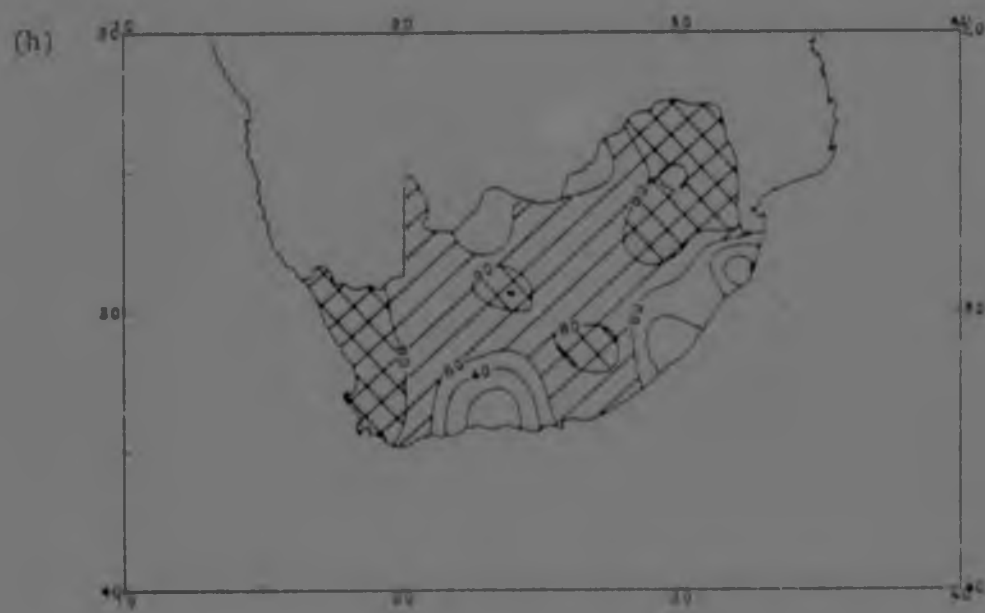


Fig 6.5 (Continued)



April



May

Fig 6.5 (Continued)



June



July

Fig 6.5 (Continued)



A dichotomous field may be observed by May (Fig 6.5h), March and April being relatively weaker fields (Figs 6.5f & g), June reverts to west coast interaction patterns (Fig 6.5i). The R^2 fields for July to September show areas of high correlation in the north-eastern regions of South Africa.

During the winter uniformly high coefficient of determination extend across most of South Africa. From this it is clear that in the winter a large amount of the variance encountered in out-of-season rainfall is associated with pressure changes over the oceanic areas. In summer, by contrast, this situation does not obtain owing to the high degree of convectively-induced rainfall over the subcontinent. Of the entire country, the south-west Cape shows the most consistent patterns of correlation between oceanic pressure and continental rainfall for both in-season and out-of-season rainfall.

6.4 SEASONAL DEPENDENCE OF RAINFALL-PRESSURE INTERACTIONS

It has already been noted that the coefficient of determination shows distinctive spatial organisation from month to month. In order to discuss the implications of this, the seasonal dependence of the above results will be considered.

The contribution of the pressure anomaly fields to rainfall variance over South Africa, presented in Fig 6.5, may be evaluated against the South African rainfall trends.

Immediately it can be noticed that with the exception of the south-west Cape, the areas of highest R^2 do not correspond in large measure to the seasonal maximum rainfall periods.

The south-west and western Cape receives most rainfall during May to August (Fig 6.1). Fig 6.5(f)-(h) shows that during this time period over 60% of the variance in rainfall is associated with sea-level pressure patterns. Highest values are found in May and June, the first months of high R^2 for this region. However, large percentages of variance (greater than 60%) of rainfall are also accounted for in the months December to April. The remaining months, October to November, show little association between the rainfall of the south-western regions of the subcontinent and the oceanic sea-level pressure patterns.

Results indicate that oceanic sea-level pressure influences the winter rainfall area, the south-west Cape, as anticipated because the tip of the subcontinent is also affected by a succession of eastward moving cyclones, associated with disturbances in the westerlies (Tyson, 1969). Since the westerlies move northwards during the winter, a good correlation between the pressure systems and rainfall was expected.

The central Cape interior, mainly the area of dual maximum rainfall months, shows associations between oceanic

sea-level pressure and rainfall over this area for the months December to February and April to July. Conspicuously absent are such associations for the months of October and March, when maximum rainfall is found.

In the summer rainfall region from May to December, that is winter to mid-summer, appreciable areas of the region are related to the pressure changes over the oceans adjacent to South Africa. Whereas for the period quoted 60 percent of the variance between pressure and rainfall is accounted for by the regression analysis, in the period January to March, that is from mid-summer to Autumn the percentage variance drops to 20 percent.

6.5 DISCUSSION

Low restriction analysis shows that high correlations are not found between periods of maximum rainfall over the subcontinent and changes in oceanic sea-level pressure. This result is not unexpected as no analysis of continental pressure changes have been made. With the exception of the south-west Cape, rainfall is largely dependent on anticyclonic moisture transportation from the Indian Ocean over the northern reaches of the country (Taliaard, 1953, Rubin, 1956; Longley, 1976).

The high restriction analysis, however, has shown an

out-of-season correlation between rainfall and the pressure fields. It is proposed that when rainfall producing pressure situations are strongly developed over the continental area, oceanic sea-level pressure changes appear to be of little importance to these features or their development. However, once they weaken, the oceanic sea-level pressure situations are related to that rainfall which does occur.

* * * *

Relationships between the pressure fields and rainfall have been discussed. Only small amounts of the variance in rainfall could be accounted for by the individual pressure fields. However, a strong association was noted between out-of-season rainfall and the principal component scores of all the pressure fields.

CHAPTER 7

CONCLUSION

In this study an attempt has been made to describe the monthly variations of oceanic sea-level atmospheric pressure. Principal components analysis of oceanic sea-level pressure over 19 gridpoints for the years 1951 to 1977 has been used to identify pressure fields over the oceans surrounding southern Africa. An investigation into the relationship between these pressure patterns and rainfall over the Republic has also been undertaken.

The specific results of the study may be summarised as follows:

- (1) Principal components analysis of oceanic sea-level atmospheric pressure indicates that three distinctive pressure patterns, designated pressure fields, may be identified for all months. These pressure fields are

- (i) a general pressure field
- (ii) a longitudinal pressure field
- (iii) a latitudinal pressure field.

Together these three account for an average of 71.4% of the total variance over all months.

- (2) The general pressure field shows a strong seasonal variation over the oceans. In summer, highest loadings occur to the south-west of Cape Town in the region of Gough Island where the subtropical ridge of zonal standing wave 1 finds its expression in the southern hemisphere. By contrast, in winter highest loadings for the general pressure field are to be found to the east of Natal over the Indian Ocean.
- (3) The longitudinal pressure field shows an east-west balance between eigenvectors of different signs. The summer pattern emphasised the Indian Ocean sector, possibly reflecting the temperature difference between the two oceans. The winter pattern suggested the importance of zonal standing wave 1 found south-west of the subcontinent.
- (4) The latitudinal pressure field appears to be associated with a *sum sole* displacement of eigenvector values during the hydrological year. High loadings found directly south of the subcontinent suggest a winter northward extension of the westerlies in a trough to the south and south-west of the subcontinent.
- (5) A stepwise multiple regression analysis with a low restriction on variables included in the regression equation produced a monthly series of rainfall -

pressure fields of interaction over the Republic.

- (i) The strongest relationship between the general pressure field and rainfall over the Republic occurred over the western sector of the Cape Province.
 - (ii) The longitudinal pressure pattern showed a strong association between loading values over the Indian Ocean and rainfall during the summer months and rainfall over large parts of the Republic.
 - (iii) As expected, the greatest interaction between the rainfall and the latitudinal pressure field is found over the western Cape during the winter months, which is the maximum rainfall season for this region.
- (6) The high restriction analysis, using a 10 percent significance level for inclusion of the principal component scores, produced a value for the coefficient of determination for each station per month. From this analysis it is evident that no strong relationship exists between oceanic sea-level pressure and periods of maximum rainfall over the Republic.

Precipitation processes have not been considered in this dissertation. Notwithstanding, relationships between rainfall over the Republic and pressure fields over the oceans surrounding southern Africa have been demonstrated. Such results support those of Tyson (1980) who has shown that

- 12 -

wet spells of the quasi 18-year oscillation on rainfall over southern Africa is strongly related to positive anomaly sea-level pressure conditions to the south-west of the subcontinent. In this region the subtropical ridge of the first zonal standing wave in the 500 mb surface has its expression in the southern hemisphere.

The present analysis has shown that during the winter months a large amount of the variance encountered in out-of-season rainfall is associated with pressure changes over the oceans surrounding the subcontinent. However, this situation is not found during the summer months as much of the continental rainfall is convectively induced and only weakly related to the oceanic pressure systems. The south-west Cape is the only region directly influenced by sea-level atmospheric circulation over the oceans. For this area consistent correlations are found between oceanic pressure and continental rainfall for both in-season and out-of-season conditions.

In any explanation of regional precipitation patterns an understanding of the general circulation is of great importance. In this dissertation changes in sea-level pressure patterns over the oceans adjacent to southern Africa have been evaluated and the foundation has been laid for further in-depth studies of the way in which the circulation of the African sector of the southern hemisphere is modulating rainfall on seasonal, annual and even decadal scales.

REFERENCES

- Barry, R G & Perry, A H, 1973: *Synoptic Climatology*, Methuen, London.
- Berlage, H P & Boer, H J, 1959. On the extension of the Southern Oscillation throughout the world during the period 1 July 1949 up to 1 July 1957. *Geof Pura e appl*, 44, 287-295.
- _____, 1960: On the Southern Oscillation, its way of operation and how it affects pressure patterns in the higher latitudes. *Geof pura e appl*, 46, 329-351.
- Chatterjee, S & Price, B, 1977: *Regression analysis by example*. Wiley, New York.
- Child, D, 1970: *The Essentials of Factor Analysis*. Holt, Rinehart & Winston, London.
- Craddock, J M, 1973: Problems and prospects for eigenvector analysis in meteorology. *The Statistician*, 22(2), 133-145.
- Craddock, J M & Flintoff, S, 1969: Eigenvector representations of the Northern Hemisphere fields. *Quart. J.R.Met Soc.*, 96, 124-129.
- Craddock, J M & Flood, C R, 1969: Eigenvectors for representing the 500 mb geopotential surface over the Northern Hemisphere. *Quart. J.R.Met Soc.*, 95, 576-593.

- Critchfield, H J, 1966: *General Climatology*. Prentice-Hall, New Jersey.
- Das, S C, 1956: Statistical analysis of Australian pressure data. *Aust. J. Physics*, 9, 394-399
- Davis, J C, 1973: *Statistics and Data Analysis in Geology*. Wiley, New York.
- de Bort, L, 1893: *Report on the present state of our knowledge respecting the general circulation of the atmosphere*. Stanford, London.
- Draper, N & Smith, H, 1966: *Applied regression analysis*. Wiley, New York.
- Gillooly, J & Dyer, T G J, 1980: Interactions between moisture deficits and maize yields, and the sub-tropical high pressure belt over South Africa. *Crop Production*, (in the press).
- Griffiths, J F (ed), 1972: *Climates of Africa*. In: Landsberg, H E. *World Survey of Climatology*. Vol 10. Amsterdam, Elsevier.
- Haworth C, 1978: Some relationships between sea surface temperature anomalies and surface pressure anomalies. *Quart. J. R. Met Soc.*, 104, 131-146.
- Jackson, S P, 1947: Air masses and the circulation over the plateau and coasts of South Africa. *J. Afr. Geog.* 29, 1-15.
- _____ 1952: Atmospheric circulation over South Africa. *S. Afr. Geog. J.*, 34, 48-60.

Kendall, M, 1973: *Time Analysis*, Griffin, London.

Kidson, J W, 1975: Eigenvector analysis of monthly mean surface data. *Mon. Wea. Rev.*, 103, 177-190.

Kutzbach, J E, 1967: Empirical eigenvectors of sea-level pressure, surface temperature and precipitation complexes over North America. *J. Appl. Met.*, 6, 791-802.

_____ 1970: Large-scale features of monthly mean northern hemispheric anomaly maps of sea-level pressure. *Mon. Wea. Rev.*, 98, 10-16.

Lamb, H H, 1959: The southern westerlies: a preliminary survey; main characteristics and apparent associations. *Quart. J. R. Meteor. Soc.*, 85, 1-11.

Longley, E W, 1975: Weather and weather maps of South Africa. S. A. Weather Bureau, Pretoria.

Lund, I A, 1962: Map pattern classification by statistical methods. *J. Appl. Met.*, 2, 56-65.

Meinardus, W, 1928: Deutsche Südpolar-Expedition 1901-1903. *Meteorologische*, Band III, Berlin, Walter de Gruyter, 133-307.

_____ 1929: Luftdruckverhältnisse und ihre Wandlungen südlich von 30° südl. Breite. *Meteor. Z.*, 46, 41-43 and 86-96.

Meinardus, W, Mecking, L, 1911: Tägliche synoptische Wetterkarten der nördlichen Breiten, von October 1901 bis März 1904. Deutsche Südpolar-Expedition 1901-1903. *Meteorologische Atlas*, Berlin, G. Reiner.

Newton, L. W. (ed.), 1972: Meteorology of the southern hemisphere.
Mon. Wea. Rev., 100, 1, American Met. Soc.

Palmer, W. N., 1971: *Handbook of weather forecasting*.
 Part 1, New Zealand Met. Office, Wellington.

Palmer, W. N., 1972: *Handbook of weather forecasting*.
 Part 2, New Zealand Met. Office, Wellington.

Palmer, W. N., 1973: *Handbook of weather forecasting*.
 Part 3, New Zealand Met. Office, Wellington.

Palmer, W. N., 1979: Truncation of the EOF Series
 in the analysis of weather data. *Mon. Wea. Rev.*, 107,
 1, 1-10.

Palmer, W. N., 1979: Empirical orthogonal functions
 of sea level height in the northern hemisphere determined
 from a 1000 day sample. *Mon. Wea. Rev.*, 107,
 1, 11-20.

Palmer, W. N., 1956: The associated precipitation and circulation
 patterns over Southern Africa. *Mon. Wea. Rev.*, 84, 5, 53-59.

Palmer, W. N. & Prohaska, J., 1956: Der Jahresgang des
 Luftdruckes auf der Erde und seine halbjährige Komponente.
Mon. Wea. Rev., 84, 1, 33-43.

Senell, J. I., 1956: On the nature and origin of the Southern
 Oscillation. *Mon. Wea. Rev.*, 84, 5, 59-69.

South African Weather Bureau, 1972: *Handbook of weather forecasting*.
 Part 1, Pretoria.

Stewart, L. J., 1973: Atmospheric pressure and wheat yield
 modelling. *Mon. Wea. Rev.*, 101, 1, 23-34.

Taljaard, J J, 1953: The mean circulation in the troposphere over Southern Africa. *S. Afr. Geog. J.*, 35, 33-45.

Taljaard, J J, 1966: Standard deviation of daily sea-level pressure and 500 mb height over the Southern Hemisphere during the IGY. *Notos*, 15, 29-36.

_____ 1967: The behaviour of 1000 - 500 mb thickness anomalies in the Southern Hemisphere. *Notos*, 16, 2-20.

_____ 1969: Air masses of the Southern Hemisphere. *Notos*, 18, 79-104.

Taljaard, J J, et al., 1959: *Climate of the Upper Air. Part 2 - Southern Hemisphere. Volume 2*, Navair, Washington.

Taljaard, J J & van Loon, H, 1960: The construction of 500 mb contour maps over the Southern Oceans. In: *Antarctic Meteorology*. Pergamon Pr., London, 96-114.

_____ 1964: Southern Hemisphere weather maps for International Geophysical Year. *Int. J. Meteor. Soc.*, 45, 88-95.

Trenberth, K, 1975: A quasi-biennial standing wave in the southern hemisphere and interrelationships with sea surface temperature. *Quart. J. R. Met. Soc.*, 101, 55-71.

_____ 1976: Fluctuations and trends in indices of the southern hemispheric circulation. *Quart. J. R. Met. Soc.*, 102, 65-75.

Tucker, G B, 1978: The general circulation of the atmosphere. In: Pittock, A B, et al, *Climatic Change and Variability*. Cambridge Univ., London.

Tyson, P D, 1969: Atmospheric circulation and precipitation over South Africa. Occ. paper No 2, *Dept. of Geography and Environmental Studies*, Univ. of the Witwatersrand, Johannesburg.

Tyson, P D, 1980: Atmospheric circulation changes and the occurrence of extended wet and dry spells over southern Africa.*

van Loon, H, 1964: Mid-season average zonal winds at sea-level and 500 mb south of 25 degrees south, and a brief comparison with the Northern Hemisphere. *J. Appl. Met.*, 5, 554-563.

1965: A climatological study of the atmospheric circulation during the IGY. Part 1. *J. Appl. Met.*, 4, 479-491.

1967a: The half-yearly oscillations in middle and high southern latitudes and the coreless winter. *J. Atmos. Sci.*, 24, 472-486.

1967b: A climatological study of the atmospheric circulation in the Southern Hemisphere during the IGY. Part 2. *J. Appl. Met.*, 6, 803-815

van Loon, H & Jenne, R L, 1972: The zonal harmonic standing waves in the southern hemisphere. *J. Geophys. Res.*, 77, 992-1003.

Veitch, L G, 1965: The description of Australian pressure fields by principal components. *Quart. J. Met. Soc.*, 91, 184-195.

*Paper presented at the meeting of the IGU Working Group on Desertification in and around Arid Lands, Fujinomiya, Japan, 25-30 August, 1980.

Vonwinckel, E, 1953: Zyklonenbahnen und Zyklogeneirische Gebiete der Südhalbkugel, *Notos*, 2, 28-36.

Vonwinckel, E, 1955: Southern Hemisphere weather map analysis: five year mean pressures. *Notos*, 4, 17-50 & 204-216.

Wahl, E, 1942: Untersuchungen über den jährlichen Luftdruckgang. *Veröff. Meteor. Inst. Univ. Berlin*, 4, 3-71.

Walker, G T, 1923: Correlation in Seasonal Variations of Weather, VII: A Preliminary Study of World Weather. *Mem. India. Met. Dept.*, 24(4), Calcutta, 75-131.

_____ 1924: Correlation in Seasonal Variations of Weather, IX: A Further Study of World Weather. *Mem. India. Met. Dept.*, 24(9), 275-332.

_____ 1928: World Weather III. *Mem. Roy. Soc.*, II(17), 97-106.

Walker, G T & Bliss, E W, 1930: World Weather IV. Some applications to seasonal forecasting. *Mem. Roy. Soc.*, III(24), 81-95.

_____ 1932: World Weather V, *Mem. Roy. Soc.*, IV(36), 53-84.

Walsh, J E & Mostek, A, 1980: A quantitative analysis of meteorological anomaly patterns over the United States, 1900-1977. *Mon. Wea. Rev.*, 108, 615-630.

Winstanley, D, 1973: Rainfall patterns and general atmospheric circulation. *Nature*, 245.

Wright, P B, 1975: An index of the Southern Oscillation. *Climatic Research Unit Report*, CRU RP4, Norwich.

APPENDIX 1

MEAN MONTHLY PRESSURE CHARTS



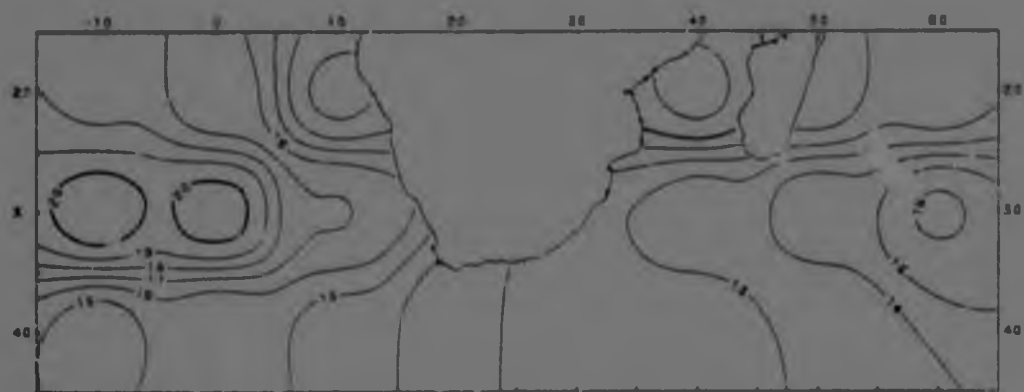
October



November



December



January



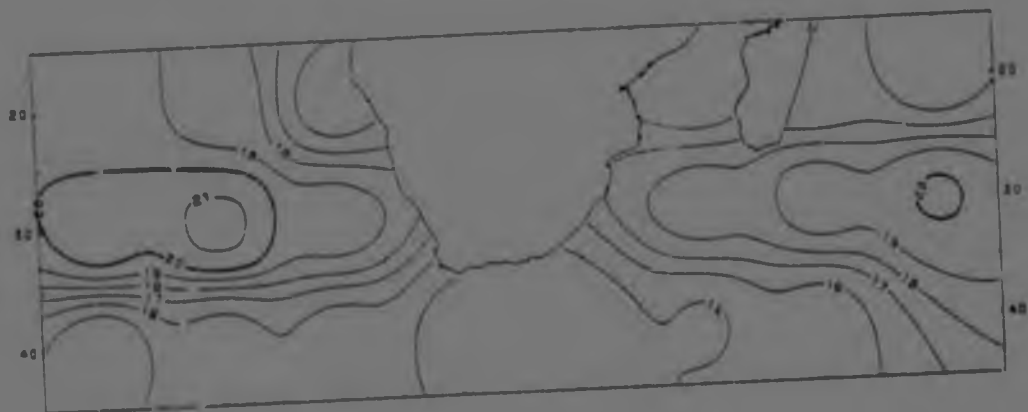
February



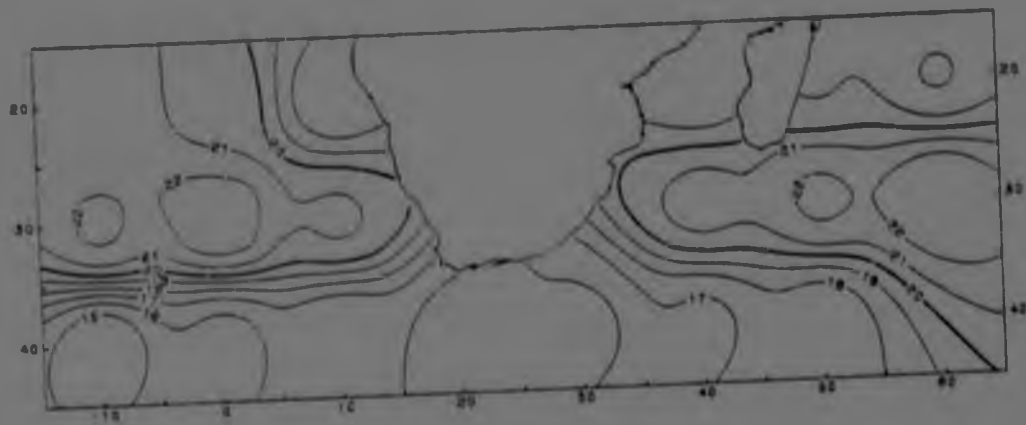
March



April



May



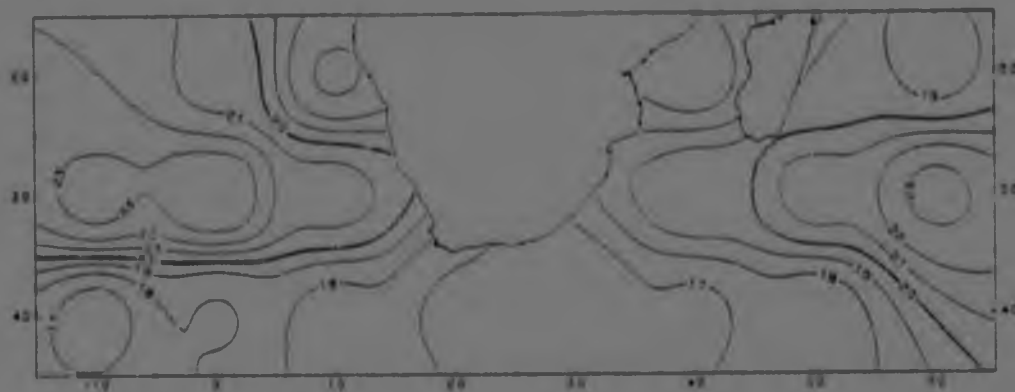
June



July



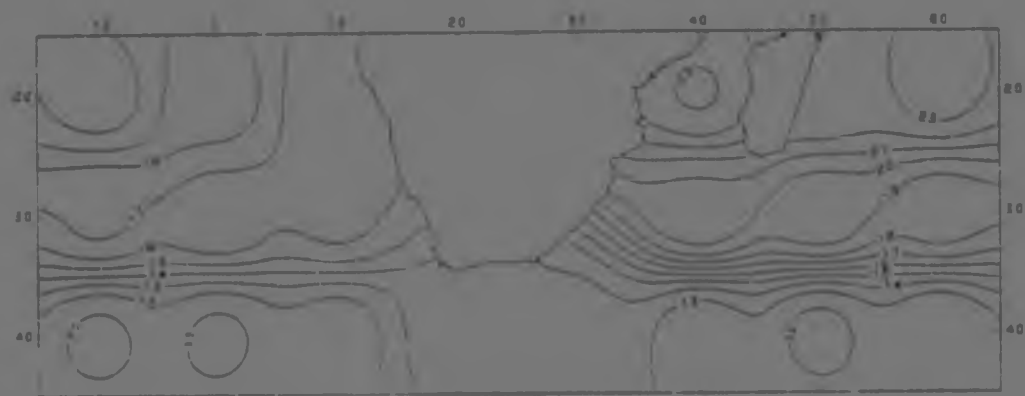
August



September

APPENDIX 2

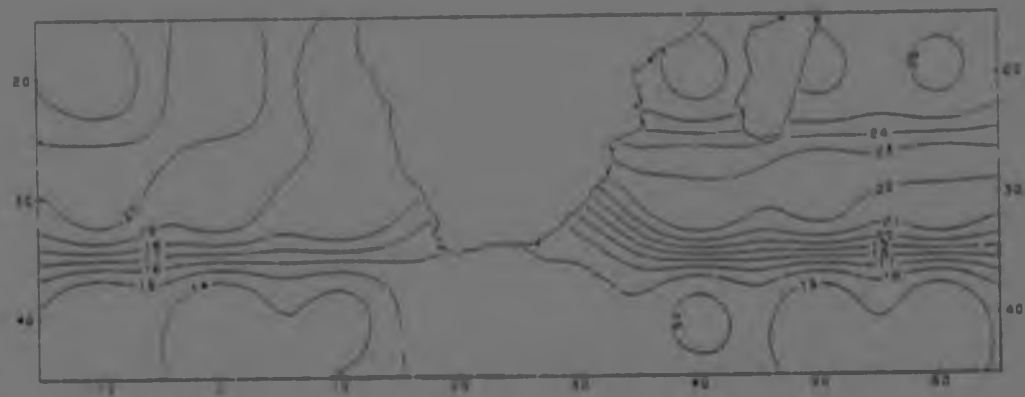
MEAN MONTHLY TEMPERATURE CHARTS



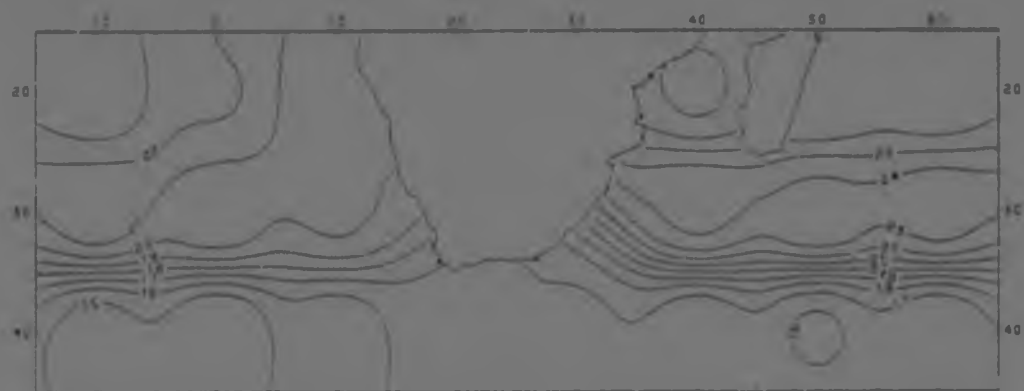
October



November



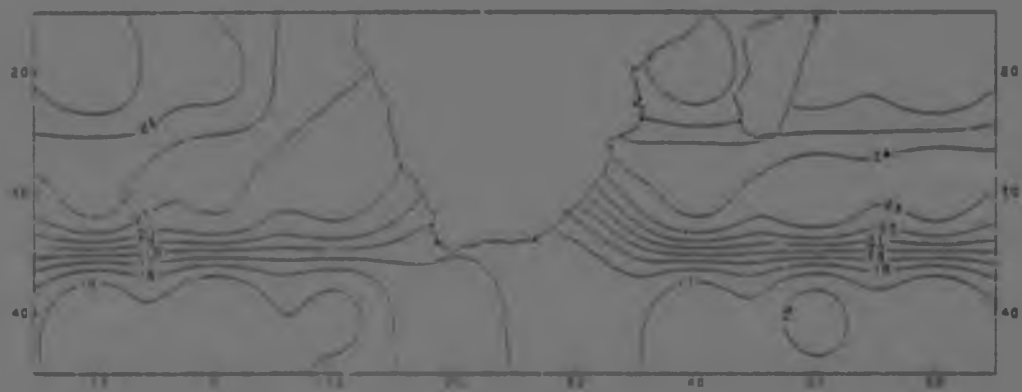
December



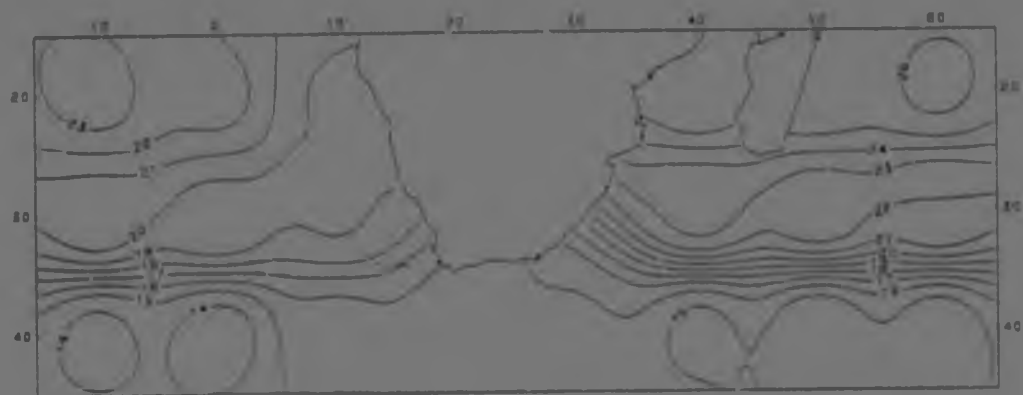
January



February



March



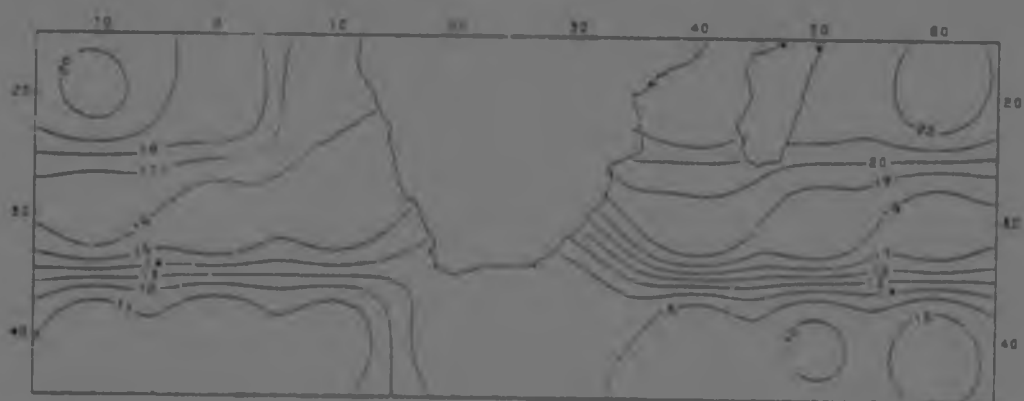
April



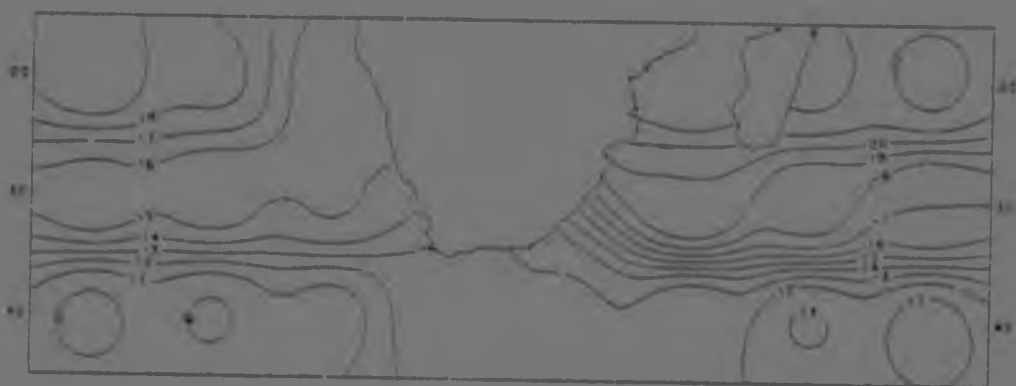
May



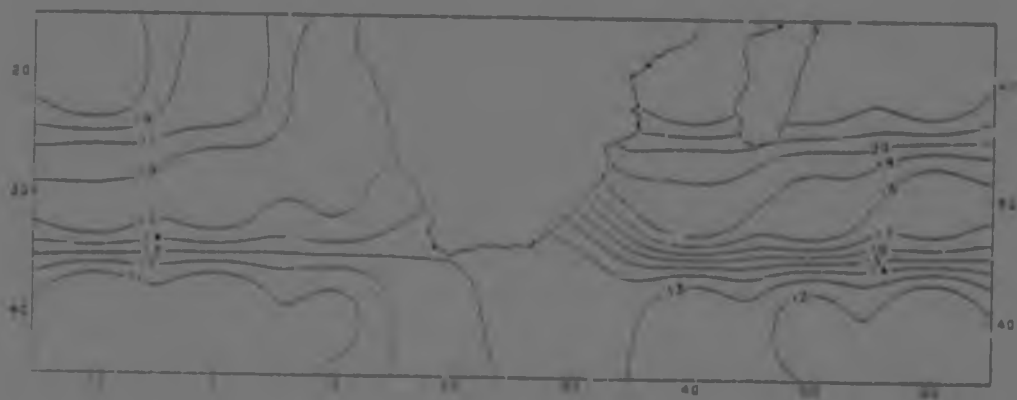
June



July

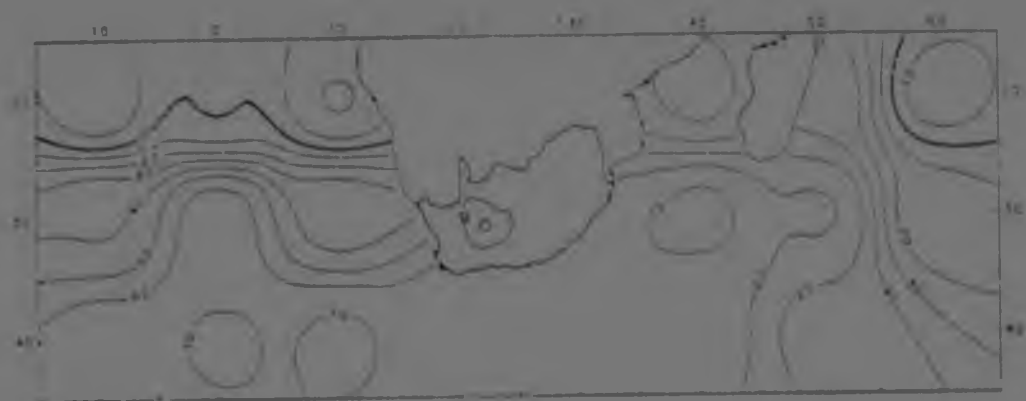


August



September

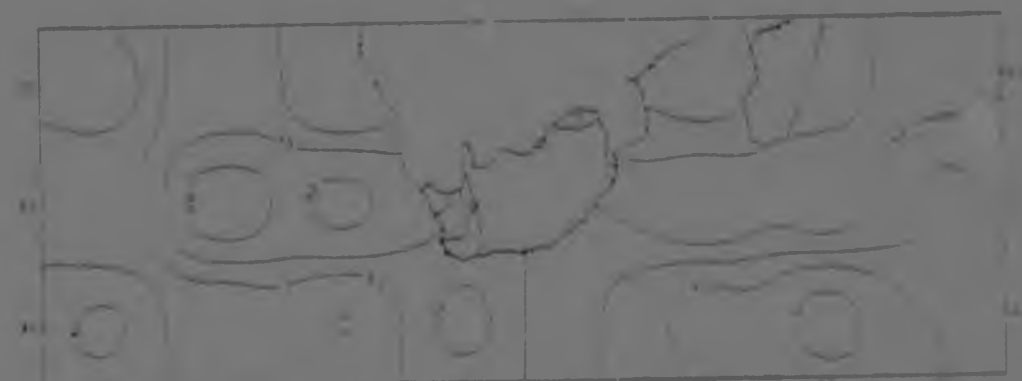
GENERAL PRESSURE FIELD AND H² CONTOURS FOR RAINFALL



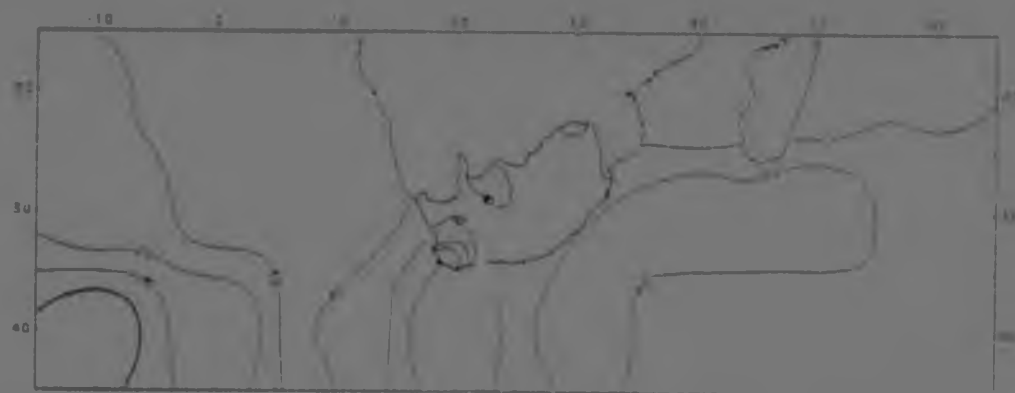
April



May



June



July



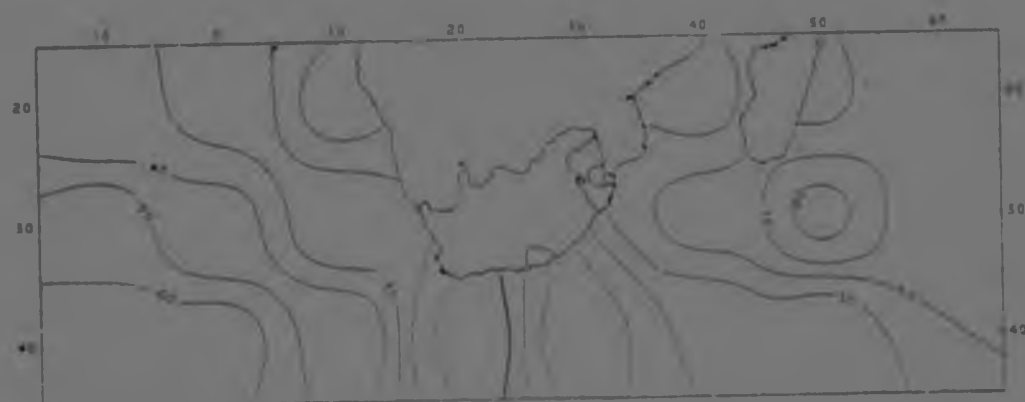
August



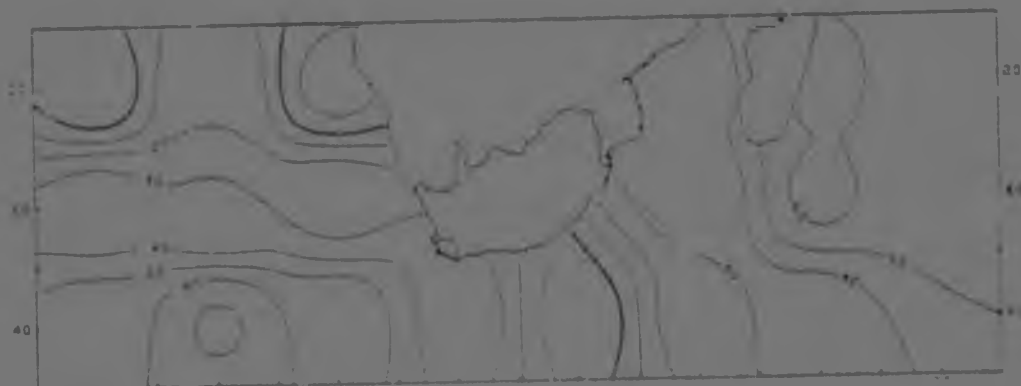
September

APPENDIX 4

LONGITUDINAL PRESSURE FIELD AND
 R^2 CONTOURS FOR RAINFALL



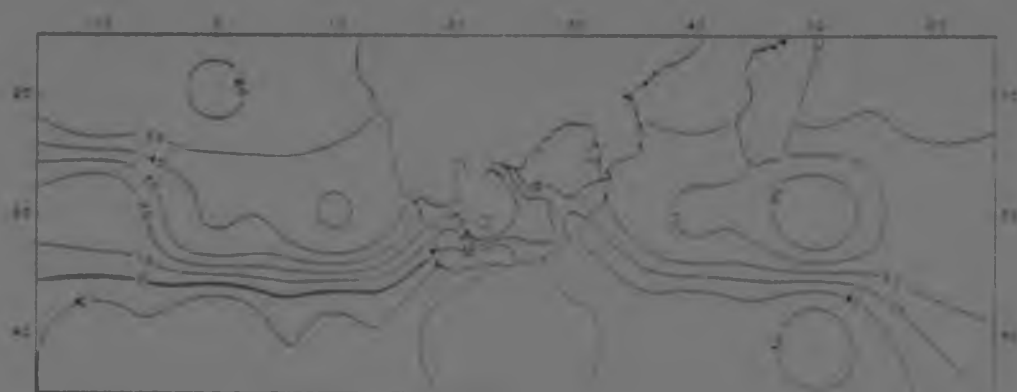
October



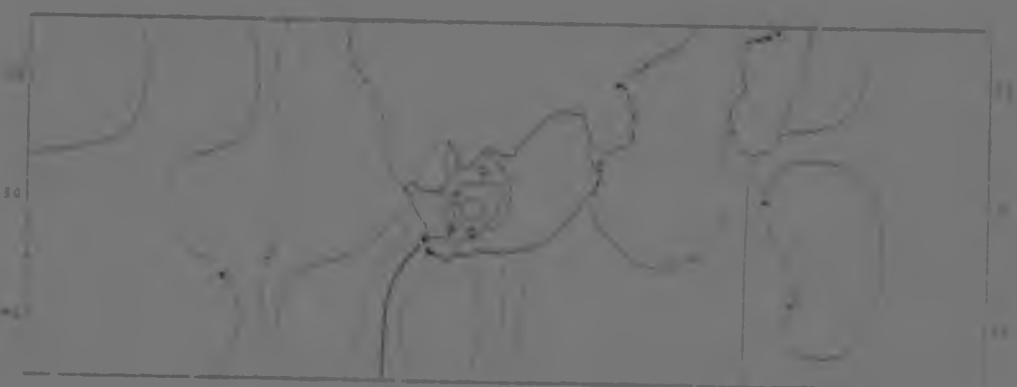
November



December



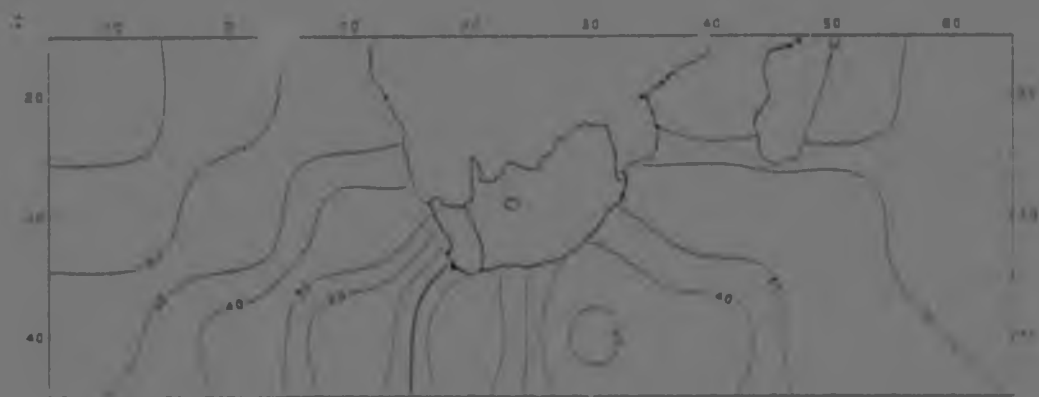
January



February



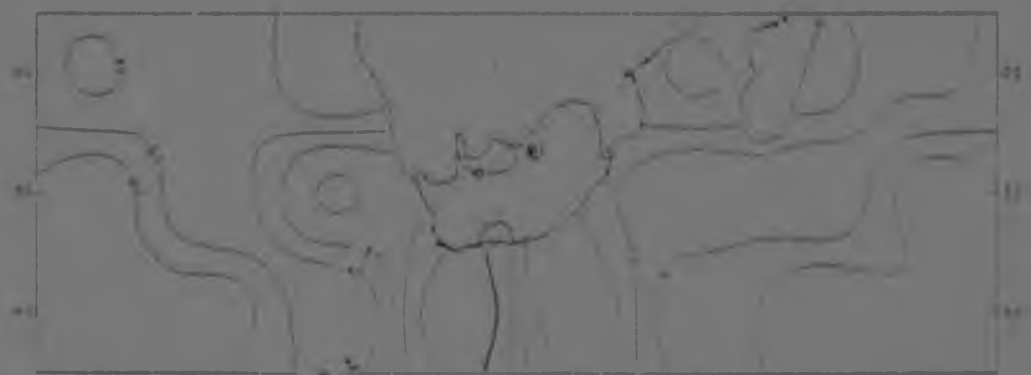
March



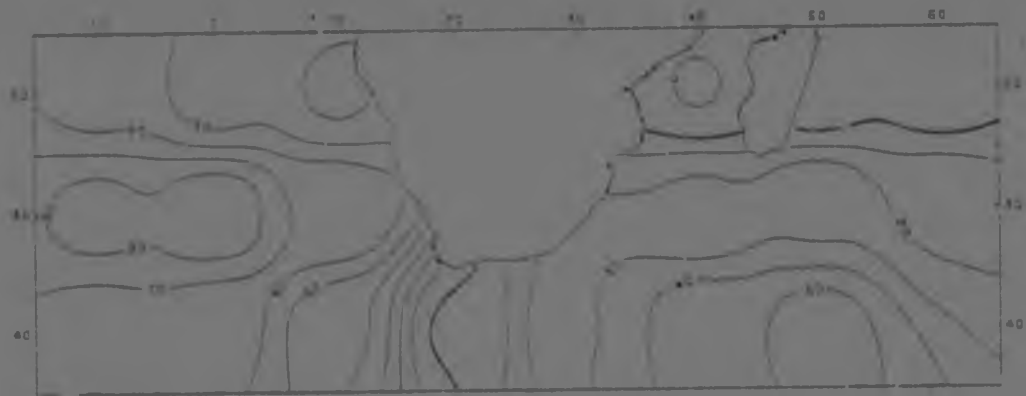
April



May



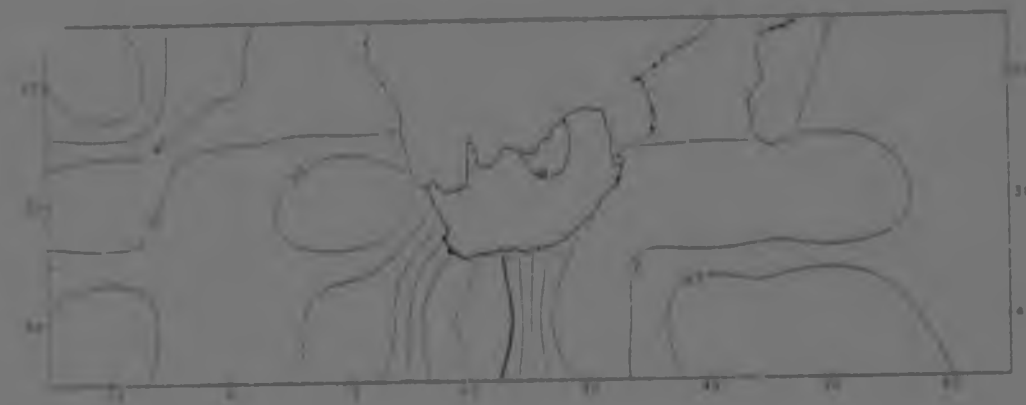
June



July



August



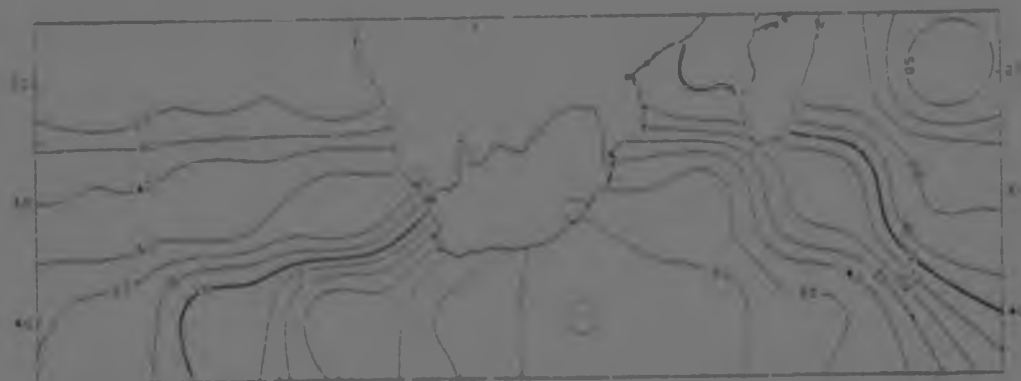
Septembe.

APPENDIX 5

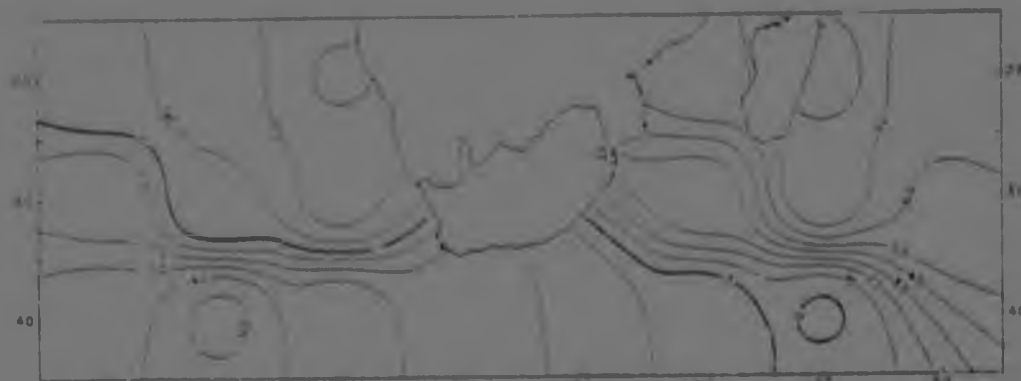
LATITUDINAL PRESSURE FIELD AND
 R^2 CONTOURS FOR RAINFALL



October



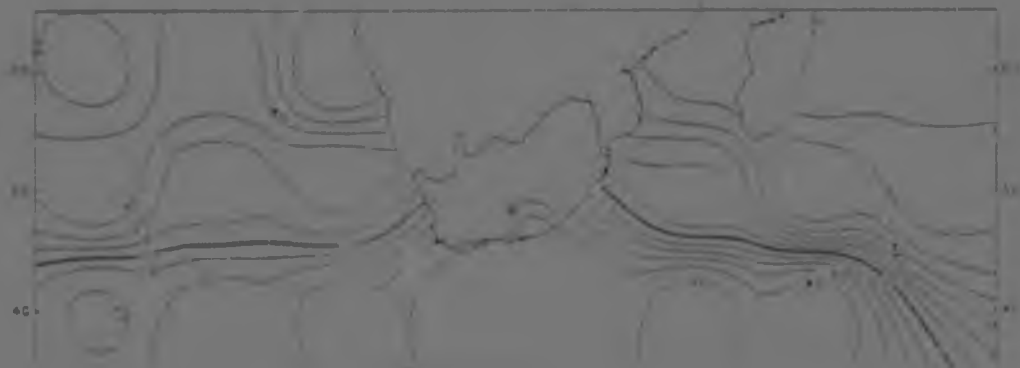
November



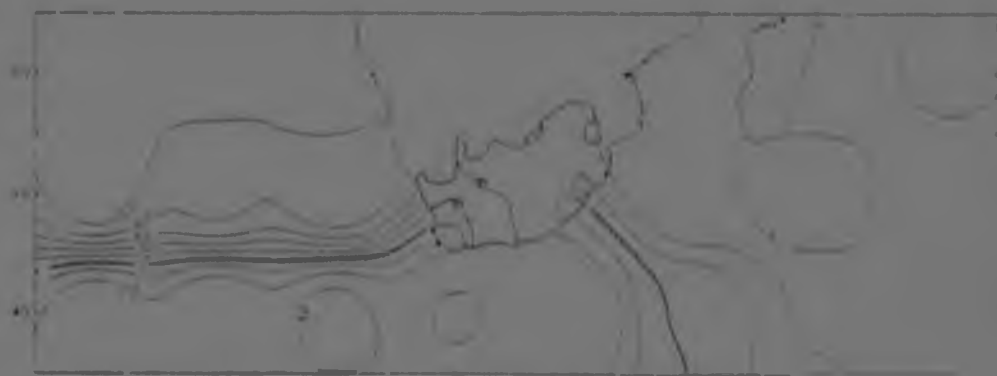
December



January



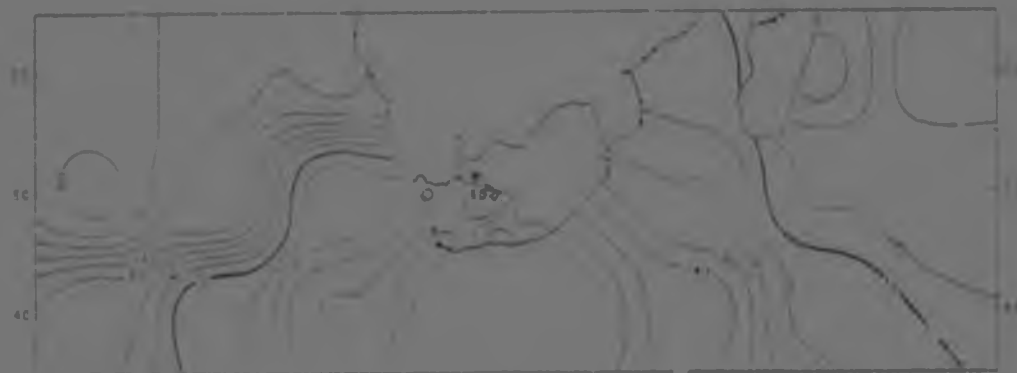
February



March



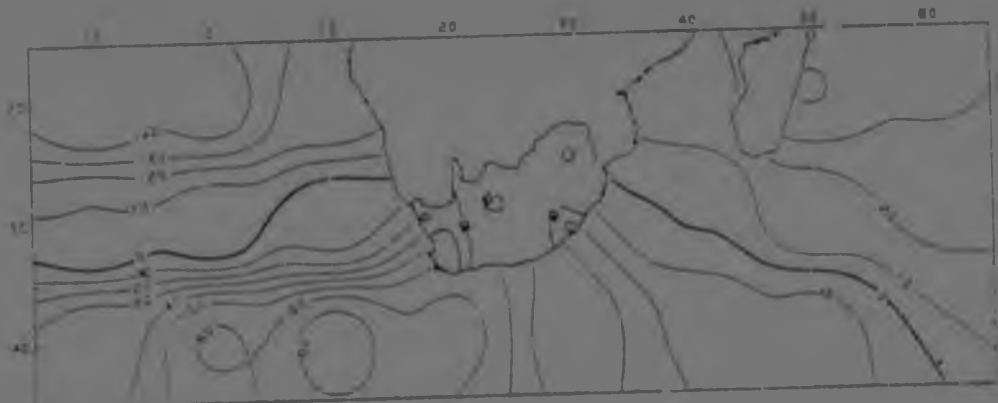
April



May



June



July

August

September

APPENDIX 6 REGRESSION EQUATIONS

JANUARY

- [1] $Y = 2.900 - 1.653E1 + 2.502E2 + 1.061E10 + 1.005E11 - 0.862E13$
 $- 1.319E16 + 0.874E18$
- [2] $Y = 4.355 - 2.145E1 + 2.311E2 - 1.080E7 + 1.551E11 + 1.883E14$
 $+ 1.314E15 - 20.052E16 - 0.808E17 + 1.339E18$
- [4] $Y = 16.070 - 5.149E1 + 8.941E4 + 2.721E5 - 2.000E7 + 1.513E11$
 $- 2.000E12 + 3.035E13 + 3.084E14 - 2.319E16 + 1.489E17$
- [10] $Y = 17.009 + 7.952E1 - 5.953E3 + 7.802E4 - 7.485E12$
 $- 10.437E15$
- [13] $Y = 53.607 + 13.567E1 + 15.334E2 - 17.868E7 - 9.026E16$
- [24] $Y = 130.475 + 27.674E1 - 21.158E15$
- [26] $Y = 119.152 + 25.670E2 + 27.831E5$
- [30] $Y = 114.624 + 18.111E2 + 25.549E3 + 20.673E6 + 18.847E12$
- [32] $Y = 155.645 + 28.278E2 - 29.839E4 - 24.534E7 + 31.503E6$
 $- 20.562E13 - 50.838E19$
- [33] $Y = 169.390 + 35.498E2 - 36.570E4 - 28.627E7 + 38.422E8$
- [35] $Y = 26.667 + 20.518E21 - 5.460E7 + 10.137E8 + 8.521E10$
 $- 5.152E13 - 7.422E15$
- [42] $Y = 75.096 + 23.365E2 - 13.737E13$
- [50] $Y = 32.154 + 37.785E5$
- [61] $Y = 113.350 - 16.960E11$
- [63] $Y = 114.803 - 17.3529E5 - 19.330E7 + 18.996E8 + 14.051E19$
- [68] $Y = 46.020 + 30.080E2 - 14.854E3 + 13.768E10$
- [71] $Y = 100.925 + 30.337E2 - 21.031E7 + 15.671E8 + 17.630E12$
 $- 16.024E13 + 18.380E16 - 15.024E19$
- [79] $Y = 60.364 + 33.508E2 - 17.392E7 + 17.310E8 + 24.937E10$
 $+ 14.850E12 - 25.077E13 + 14.356E16$
- [84] $Y = 106.564 - 13.215E7 + 12.025E8 + 18.224E12 - 13.238E13$
 $+ 17.435E16 - 11.724E17$
- [93] $Y = 104.142 + 25.435E8 + 21.289E10$

FEBRUARY

- [1] $Y = 6.743 + 1.244E7 - 4.104E10 - 3.466E14 + 9.836E16$
- [2] $Y = 8.005 - 5.341E1 - 2.492E3 + 5.867E6 - 3.348E8 + 2.232E9$

- +3.752E11+6.102E16-3.798E18
 [4] Y=19.076-11.482E1-10.112E3+7.853E4+10.321E6+5.703E7
 +7.817E11+13.393E16-8.590E18
 [10] Y=23.826-7.621E4-12.301E10
 [13] Y=60.491-9.786E1-16.229E2-11.575E4+7.553E16
 -10.981E18
 [24] Y=11.832-14.626E1+16.172E11-20.216E18
 [26] Y=13.154-18.483E3-35.658E6-20.422E7-25.631E10
 -26.932E12-23.428E13+22.629E14-24.673E17
 [30] Y=120.498+10.729E2+8.795E3-24.947E6-11.304E8
 -12.364E10+14.560E11
 [32] Y=148.669-36.927E6-21.954E8-18.905E10-17.589E13
 +29.512E14-35.586E17+19.427E19
 [33] Y=145.951+29.309E11
 [38] Y=17.905-2.928E1-4.193E2+15.980E3-17.404E4+2.772E7
 -3.417E9+11.507E11+4.059E12-3.719E13+4.670E17
 -4.378E19
 [42] Y=84.489-11.831E2-20.303E6-14.159E9-13.383E10
 +8.800E11+15.129E13+9.065E18
 [50] Y=75.432-15.819E5-15.105E8-15.330E10+12.421E11
 [61] Y=95.320
 [63] Y=97.326+11.049E2+15.328E11-12.112E12+14.992E19
 [68] Y=53.552+17.434E3-21.261E4+14.035E11-7.693E19
 [71] Y=102.108+8.854E3-23.033E4-29.137E6-11.150E9
 -22.817E10+10.998E11-10.331E12+13.273E13+7.725E14
 [79] Y=65.311+11.372E3-14.740E4+10.318E7+16.337E11
 [84] Y=93.104-20.332E4+16.479E7
 [93] Y=89.534-18.942E4-22.451E5+18.051E11+15.664E16

MARCH

- [1] Y=9.897+3.493E4-3.345E16
 [2] Y=9.979+4.406E3-3.634E9-3.442E16+3.514E19
 [4] Y=22.999-9.568E2+10.146E3+4.367E8-6.0894E9
 -5.311E16+3.712E19
 [10] Y=30.637+11.777E2-6.161E16
 [13] Y=77.155+17.765E1-23.814E3
 [24] Y=134.181+23.741E2-22.693E3+36.744E5+44.147E8
 +18.919E11-28.547E14+21.495E15-26.5459E19
 [25] Y=113.528-29.152E3+22.722E8+17.903E9-29.113E10
 +16.527E13+16.883E15-25.350E18
 [30] Y=93.055-23.378E3+23.662E5-20.132E14
 [32] Y=93.320-17.206E3-16.353E11+16.274E15
 [33] Y=94.759+22.351E4+15.753E15
 [38] Y=50.570+24.513E2
 [42] Y=77.475+18.356E2-17.875E3-12.318E14
 [50] Y=42.507-16.614E3+15.903E4+10.636E8+12.696E19

+9.032E15+9.648E16
 [61] Y=65.994-9.734E3+12.985E16+9.280E17
 [62] Y=72.969-13.362E3-5.688E10+11.913E15+17.232E16
 [68] Y=59.176+20.702E2-16.364E3
 [71] Y=85.568-13.703E3+14.316E4
 [79] Y=76.029+17.292E2-24.945E3+24.079E4+26.353E10
 +23.118E17-17.952E19
 [84] Y=78.652E2-13.490E3-11.540E11
 [93] Y=71.667+20.399E2-12.416E3-13.371E10-18.299E11
 +14.678E12

APRIL

[1] Y=16.505+5.675E2-6.667E5-4.753E6+7.454E8.4.461E10
 -4.085E14
 [2] Y=27.524+8.379E2-5.794E5-7.618E6+10.508E8-8.40E9
 +8.330E16
 [4] Y=60.187-11.108E1+14.070E2+22.576E3+14.290E4
 -12.022E6-11.770E7
 [10] Y=29.920
 [13] Y=46.090-12.752E3-13.621E14
 [24] Y=80.526-19.644E3-19.337E11+26.346E12
 [26] Y=102.340+17.057E1-25.712E3+19.414E4+19.538E10
 +22.073E16
 [30] Y=60.176-13.934E3+9.938E12-9.818E14
 [32] Y=68.000
 [33] Y=65.200
 [36] Y=25.573+10.697E1-10.271E3-8.632E5+6.428E12
 [42] Y=43.753-5.514E14
 [50] Y=30.696+7.666E10+6.571E13
 [61] Y=52.553-7.398E3+7.616E4-9.443E5+5.832E6-6.268E11
 +5.761E12-12.860E14+7.671E17
 [63] Y=60.750-7.215E3+11.002E10-6.835E14+8.190E16
 +12.326E17
 [68] Y=36.583+6.949E1-7.360E2-7.371E5-9.384E18
 [71] Y=65.072+10.556E40+11.989E8-10.242E14
 [79] Y=42.538+5.172E1-5.146E5-5.971E6+13.989E8+5.707E10
 -5.245E14+9.587E16
 [84] Y=67.333-14.556E3+13.686E4-7.687E5+10.737E6
 -6.232E7+11.558E8+7.935E10-6.432E11+8.380E13
 -8.745E14+16.670E17-7.542E18
 [93] Y=66.779-15.144E3+22.361E4+15.578E5+18.688E10
 +18.210E17

MAY

- [1] $Y=25.431-14.449E1+12.860E2+8.910E3-4.364E6$
- [2] $Y=45.144-20.431E1+17.991E2-7.225E3-7.042E4+12.621E5$
 $+6.809E11-8.358E12$
- [4] $Y=106.780-33.389E1+36.825E2-19.395E3+73.436E5-12.799E8$
 $-10.985E12$
- [10] $Y=31.144+7.499E6$
- [13] $Y=54.842+17.073E2-17.661E4+14.806E6+11.505E9-10.912E12$
 $+11.209E14+13.676E15$
- [24] $Y=63.703-27.014E1+24.605E6$
- [26] $Y=75.994+29.595E12$
- [30] $Y=28.591-21.248E1+22.042E5+14.668E8+16.117E19$
- [32] $Y=29.557-5.194E2+12.471E5+5.774E7+11.779E8-4.659E9$
 $+6.935E11+9.352E12+5.645E14-9.905E15+8.703E16$
- [33] $Y=26.200-4.852E1+1.848E3+8.906E4+8.326E5+3.047E6$
 $+4.808E7+4.065E8-2.757E10+5.778E12-2.462E13$
 $-3.502E14+9.950E16+6.373E18$
- [38] $Y=15.663+7.737E2-3.046E4+3.058E8+5.213E11$
- [42] $Y=24.353+3.353E2-9.845E4+4.883E6+3.472E7+4.714E8$
 $+3.782E10+5.887E11-8.990E12+6.570E14$
- [50] $Y=8.795-5.259E1+1.763E3+3.133E4-1.813E5+2.276E6-2.789E7$
 $+3.630E11+3.753E12-4.426E14+2.582E16+2.774E18+2.520E19$
- [61] $Y=18.801+5.132E3+3.241E4+6.822E5+7.140E8-2.871E9$
 $+6.404E11-6.024E13-3.144E17$
- [63] $Y=18.478+3.731E2+9.779E4+4.054E5+7.290E6+4.085E8$
 $+6.065E12-6.427E14-3.832E17$
- [68] $Y=14.371-6.339E1+2.131E2+3.140E3+4.132E5+2.429E8$
 $+5.403E11-4.766E16+5.642E18$
- [71] $Y=24.472+5.908E2-5.684E4+5.145E6+11.445E11+6.682E19$
- [79] $Y=17.434-5.718E1+5.791E8+5.786E11+6.068E19$
- [84] $Y=20.454+8.786E3+4.755E7+8.354E8+6.865E11+3.778E12$
 $-3.231E13-4.518E18$
- [93] $Y=15.667-7.039E1+7.432E3+7.256E5+7.222E11$

JUNE

- [1] $Y=31.895-13.418E1-4.187E2-7.335E3+7.759E5+4.150E6$
 $+5.485E7+4.415E11+4.063E13+5.726E14-7.087E15$
- [2] $Y=58.922-20.538E1-4.922E2-9.327E3+15.422E5+13.972E6$
 $+11.184E7+11.910E11+17.395E14-15.803E18-7.578E19$
- [4] $Y=126.927-27.389E1-32.692E3+19.875E5-21.753E16$
- [10] $Y=28.629-5.952E2+9.815E14$
- [13] $Y=34.407-5.596E1-5.683E2-19.033E11+10.915E12+5.957E17$
- [24] $Y=34.434+25.358E12+20.125E19$
- [26] $Y=31.286+27.510E3+15.534E8+22.363E13+16.848E18$
- [30] $Y=14.376+5.057E3+6.338E4+8.101E15$
- [32] $Y=17.787+6.054E5+6.878E8-2.531E12+11.886E13$
- [33] $Y=17.780+5.722E8-11.970E12+8.462E13+8.387E14+6.038E15$

- 4.970E17
 [35] $Y=7.606+1.919E1-2.316E4+3.903E6+4.763E14+2.390E16$
 $-2.824E18$
 [42] $Y=16.215+2.602E14-4.195E7+5.286E8+2.926E9-4.115E11$
 $+4.262E14+9.102E15-7.297E18+3.238E19$
 [50] $Y=5.712+3.371E1+1.660E2+2.535E5+1.838E6+2.252E7-3.041E9$
 $-1.500E10-2.545E11+2.466E13-3.305E16$
 [61] $Y=6.103+4.325E3+2.289E5+3.979E6+3.307E7+4.983E13$
 [68] $Y=7.027-2.585E2+4.516E14-3.883E18+3.014E19$
 [71] $Y=13.193+3.212E4+5.919E8-4.827E11+3.615E13+7.164E14$
 $+3.183E19$
 [79] $Y=8.123-6.006E2+4.425E6-4.168E9-4.413E12+5.475E14$
 $+4.061E19$
 [84] $Y=7.360$
 [93] $Y=5.437+5.015E1-4.091E4-5.803E3+5.308E13+4.405E19$

JULY

- [1] $Y=25.172-5.952E3+5.430E4-10.962E5-6.971E9+5.227E10$
 $+7.704E17$
 [2] $Y=45.422-7.795E1-11.351E3+7.929E4-8.111E5+6.210E6$
 [4] $Y=108.744-29.033E1-24.728E3+16.320E4-16.485E5$
 $-10.334E8$
 [10] $Y=27.782-11.310E6-19.305E9-8.731E10+21.834E14$
 $+5.704E16+13.773E17-10.829E19$
 [13] $Y=29.503+8.593E2+7.828E3-5.425E4-6.586E5-5.775E6$
 $-6.129E12+6.930E13+7.723E14+6.367E15$
 [24] $Y=30.179+16.264E3-13.316E5+10.628E8-9.537E12$
 $+16.758E13+10.107E14$
 [26] $Y=50.190+16.878E3-21.335E5-21.187E7+22.647E13$
 $-14.053E16-14.356E17$
 [30] $Y=13.370+5.268E3-6.523E5-5.946E7+7.885E13-6.540E17$
 [32] $Y=13.660+6.469E4-13.062E5+5.226E6-11.156E7-6.515E17$
 $-7.257E18$
 [33] $Y=11.353-8.637E5-7.174E7-5.336E17-4.707E18$
 [38] $Y=6.470+2.313E3-4.221E5-2.887E10+3.081E13-4.438E14$
 [42] $Y=3.354-4.356E5+4.424E8$
 [50] $Y=2.120+1.005E1-0.995E13-0.912E17$
 [61] $Y=6.116-3.962E2+8.026E4-17.806E5-9.588E7-6.488E8$
 $+5.025E18-4.344E13-7.635E18$
 [63] $Y=4.652+2.215E3-2.437E5-1.776E7+1.986E11-3.786E17$
 [68] $Y=3.105+2.822E1-1.868E2+2.201E3-4.574E5-2.665E6$
 $-2.460E11+3.608E17-1.322E18$
 [71] $Y=3.400+4.363E1-10.505E5-6.922E14+6.281E19$
 [79] $Y=2.801+2.635E1+2.175E3-3.514E5+3.244E17$
 [84] $Y=4.654-4.565E5$
 [93] $Y=5.236-6.177E13$

AUGUST

- [1] $Y=30.568-9.273E1-9.468E2+9.762E3$
- [2] $Y=50.447-15.729E1-14.390E2+11.287E3+8.755E11$
- [4] $Y=129.468-31.5.3E1+15.919E3+22.288E4-18.625E17$
- [10] $Y=43.678+12.720E4-13.028E17+10.112E18$
- [13] $Y=49.201+13.671E2+14.483E3-22.231E8-15.885E10$
 $+18.417E11+14.093E19$
- [24] $Y=48.914+12.706E2-11.938E7-18.435E8-30.418E19$
- [26] $Y=50.242-18.142E7$
- [30] $Y=31.986+9.766E1-9.039E5-12.560E7-11.240E8$
 $-10.334E10$
- [32] $Y=18.984+7.630E1-15.522E7-5.587E8+6.976E9-7.610E16$
 $+6.007E19$
- [33] $Y=14.436+5.961E1-12.620E7+6.146E9$
- [38] $Y=6.008+3.341E3$
- [42] $Y=17.644+10.857E3-10.137E8+15.288E11+11.756E19$
- [50] $Y=1.936+0.993E1-2.063E7+1.406E8+1.257E10$
- [61] $Y=10.363+2.745E1-4.619E4-3.680E5-2.624E7-4.695E8$
 $-3.395E12-5.288E14+5.056E15-3.386E18$
- [63] $Y=7.955-7.649E7$
- [68] $Y=5.013-3.515E1-3.206E5+3.918E10+3.965E11-3.429E17$
- [71] $Y=12.490-4.539E5+5.605E11-5.351E14+6.601E15$
 $-5.715E17$
- [79] $Y=4.922-2.812E1-3.073E5+4.139E10+3.845E11-3.653E17$
- [84] $Y=4.131-2.298E5-2.177E7$
- [93] $Y=3.153+2.566E1-3.106E18$

SEPTEMBER

- [1] $Y=9.026-2.569E3-4.155E4$
- [2] $Y=16.374-4.389E1-3.714E3-4.605E4-3.028E19$
- [4] $Y=51.601-14.874E1-7.958E3$
- [10] $Y=20.073-6.122E19$
- [13] $Y=67.538+31.765E5+13.895E6+23.995E12-20.861E19$
- [24] $Y=80.000+20.240E6$
- [26] $Y=71.911-20.345E5+23.443E6+18.418E13-24.136E15$
- [30] $Y=52.467-13.449E5+19.072E6-13.935E10+13.370E13$
- [32] $Y=44.432-13.615E5+12.666E6+13.833E13-12.792E15$
 $+16.899E16-8.936E17+14.363E19$
- [33] $Y=39.665+11.800E8-12.215E15+17.372E16+13.334E19$
- [38] $Y=2.640$
- [42] $Y=22.159-2.823E1+4.241E2+7.459E4+7.392E5+6.315E6$
 $-2.675E7+3.640E8+5.128E9-5.957E10+3.841E12+2.245E13$
 $-4.231E14+3.999E15$
- [50] $Y=9.531+6.988E16$
- [61] $Y=28.111-9.849E2-5.327E3-11.658E5+17.973E6+4.553E8$
 $+7.726E9+9.559E13-14.522E15-7.695E17$

- [65] $Y=27.660-7.501E2+6.125E4-6.108E5+3.982E7+13.421E8$
 $+6.924E11-5.066E12+6.767E13+4.645E16-4.116E17$
 $-6.354E18+7.252E19$
- [66] $Y=2.212+2.927E6+1.389E13-2.143E15-1.474E17$
- [71] $Y=22.001-6.664E2+7.555E4+7.683E6+13.087E8-14.538E10$
- [79] $Y=2.475+5.159E6-2.459E11+3.117E13-3.210E15$
- [84] $Y=11.516-7.212E2+4.598E4-6.235E6+7.808E8+4.785E13$
- [93] $Y=12.923-7.710E2+4.678E4-4.827E5+6.383E6+4.965E8$
 $+4.908E13+4.975E14-3.362E15-4.106E18$

OCTOBER

- [1] $Y=12.604-4.023E3-3.340E17$
- [2] $Y=18.146-5.536E1-5.852E3-4.256E6$
- [4] $Y=54.068-15.320E3-13.143E6$
- [10] $Y=25.281+9.894E1+6.573E5$
- [13] $Y=61.237+26.109E1+16.407E2-14.204E4+32.057E5$
 $+10.726E6+20.357E16+13.487E19$
- [24] $Y=120.939+19.294E3+17.418E4+14.452E5-27.261E6$
 $-10.613E7-21.114E8-21.957E11-22.702E13-20.547E17$
 $+19.978E18+21.359E19$
- [26] $Y=107.564+11.302E1-23.711E2-15.632E6-12.849E8$
 $-15.166E13-15.474E17+8.708E18+21.375E19$
- [30] $Y=85.553-7.873E2-11.682E7-12.451E8-12.077E13$
 $-12.777E17+19.159E19$
- [32] $Y=92.144-17.350E2-16.613E11$
- [33] $Y=77.950-11.167E1-14.571E2-11.170E7-9.604E9+9.610E10$
 $-8.876E11+8.642E15$
- [38] $Y=12.048+5.141E1+3.947E14$
- [42] $Y=37.387+5.689E1-3.605E7-8.954E12-8.480E17$
- [50] $Y=33.542+10.127E6-9.903E9+8.841E10+9.454E18$
- [61] $Y=75.360$
- [63] $Y=70.133-9.409E2-10.086E3-13.8209E7+11.996E10$
- [68] $Y=17.141-4.334E3-5.759E5-5.238E7$
- [71] $Y=51.138-19.558E3-12.213E7-13.024E14+10.636E15$
- [79] $Y=17.074-7.269E9$
- [84] $Y=44.325-12.730E3-7.162E5-10.828E7+7.465E10-5.897E14$
 $+12.103E15$
- [93] $Y=40.390+10.551E15$

NOVEMBER

- [1] $Y=7.352+3.221E2+3.845E15+4.329E18+2.914E19$
- [2] $Y=10.995+5.134E15$
- [4] $Y=26.342+7.838E3$
- [10] $Y=22.414-6.567E8+8.376E15$
- [13] $Y=56.424+12.575E1-12.068E8-11.350E14$
- [24] $Y=127.364-15.082E2-11.647E8-16.891E9+15.515E13$

- 11.292E14
- [26] $Y=113.611+10.918E1-20.301E3-29.972E6+15.768E7$
 $-17.152E8+35.934E11+20.377E12$
- [30] $Y=116.389-7.052E2-10.561E6-13.889E9+8.207E13$
 $-7.041E14+10.123E15+6.202E17-4.862E19$
- [32] $Y=132.789+10.567E5-32.384E6-17.830E8+15.541E12$
 $+12.222E16+16.834E18$
- [33] $Y=126.250-32.185E6-15.414E8+15.802E12+23.394E18$
- [38] $Y=18.160-4.442E9+4.962E15+5.846E17$
- [42] $Z=57.425+9.752E1-15.729E8-8.972E9+14.898E13+8.545E15$
 $+7.527E17$
- [50] $Y=57.348+13.448E1-12.598E8-9.175E16+14.541E18$
- [61] $Y=112.667-17.351E6$
- [63] $Y=127.960+16.548E1-9.376E3-27.564E6-13.930E9$
 $+6.914E11+17.099E12+19.987E18$
- [68] $Y=25.048-5.936E9+7.828E15$
- [71] $Y=75.269-13.833E8-18.542E9+12.456E13+9.928E14$
 $+22.450E15+8.118E17$
- [79] $Y=29.552-10.259E8+6.284E10+6.168E14+7.089E15$
 $-8.187E19$
- [84] $Y=31.923+8.399E1-9.089E2-10.062E9+14.466E15$
- [93] $Y=77.752+12.853E1-18.922E8$

DECEMBER

- [1] $Y=5.409-3.743E4+3.695E7-7.229E8+3.138E14$
- [2] $Y=7.952-3.110E6+3.174E11+3.038E14$
- [4] $Y=19.290-6.624E1-5.440E5+5.710E7$
- [10] $Y=18.092+3.943E2-9.481E6+3.111E7+4.330E14-2.835E15$
 $-5.195E17-4.071E18$
- [13] $Y=45.100-10.187E4-9.785E5-23.856E6-11.151E10$
 $+9.104E13$
- [24] $Y=126.214+14.033E1-13.892E4-11.257E6-24.036E7$
 $+18.914E12+20.659E13+9.524E16-17.626E17-11.387E19$
- [26] $Y=116.299+25.873E1-40.679E6-31.512E7+28.861E10+20.335E12$
 $+29.610E16$
- [30] $Y=126.101+16.569E1-7.749E3-18.077E6-13.585E7$
 $+15.218E10+8.280E13+12.084E16$
- [32] $Y=136.062+27.295E1-23.522E2-40.681E4$
- [33] $Y=152.599+25.477E1-10.334E2-25.615E4-12.495E6$
 $-22.419E9+14.696E10+13.622E11-20.038E14+28.046E17$
 $-14.670E19$
- [38] $Y=19.976+3.863E1+8.027E3-5.407E4-2.875E5-8.125E6$
 $-5.171E8-10.161E9+2.673E10+3.114E11-2.781E16$
 $-3.666E18$
- [42] $Y=71.594-14.717E4-15.616E6+9.156E12+11.812E16$
 $+13.619E17$
- [50] $Y=79.922-13.771E4-12.880E6-12.764E8$

- [61] $Y=110.64J-12.597E2-15.537E6-13.643E7$
[63] $Y=132.551+24.763E1+12.621E5+9.024E13-11.964E14$
 $+9.285E15$
[68] $Y=35.066+8.536E1+11.797E3-9.054E4-8.597E6-11.656E9$
 $+16.063E11-7.201E18$
[71] $Y=82.996-9.717E2-16.040E6+14.250E16+9.312E19$
[79] $Y=50.832+11.543E1+13.508E3-6.230E5-7.562E6-17.632E9$
 $+13.976E10+22.694E11+10.683E17-14.161E18+13.026E19$
[84] $Y=94.913-8.322E2-19.150E4-13.337E6-12.344E14$
 $+8.043E16$
[93] $Y=88.454+13.515E3-18.431E4$

APPENDIX 7

PRINCIPAL COMPONENTS ENTERED INTO REGRESSION EQUATIONS
(PER RAINFALL DISTRICT)

	Rainfall Districts																			
	1	2	4	10	13	24	26	30	32	33	38	42	50	61	63	68	71	79	84	91
1																				
2																				
3																				
4																				
5																				
6																				
7																				
8																				
9																				
10																				
11																				
12																				
13																				
14																				
15																				
16																				
17																				
18																				
19																				
R ² (%)	83	85	95	63	59	38	32	60	62	51	38	34	21	15	55	55	71	70	45	30

January

	Rainfall Districts																			
	1	2	4	10	13	24	26	30	32	33	38	42	50	61	63	68	71	79	84	91
1																				
2																				
3																				
4																				
5																				
6																				
7																				
8																				
9																				
10																				
11																				
12																				
13																				
14																				
15																				
16																				
17																				
18																				
19																				
R ² (%)	73	74	75	62	66	43	35	74	74	72	26	23	24	1	28	23	70	57	25	13

February

		Rainfall Districts																															
Principal Components		1	2	4	10	11	24	26	30	32	33	38	42	50	41	43	58	71	79	84	92												
	1						X																										
	2				X	X	X					X	X					X		X	X	X											
	3			X	X		X	X	X	X				X	X	X	X	X	X	X	X	X											
	4		X									X								X	X												
	5							X		X																							
	6																																
	7																																
	8				X			X	X							X																	
	9			X	X				X								X																
	10								X										X									X					
	11							X			X																		X	X			
	12																															X	
	13										X																						
	14							X		X					X																		
	15							X	X		X	X				X		X															
	16		X	X	X	X										X	X	X															
	17																	X											X				
	18									X																							
	19			X	X				X																				X				
	Pr(%)	23	16	12	54	26	10	12	50	46	24	27	45	45	38	63	50	73	78	90	92												

March

		Rainfall Districts																															
Principal Components		1	2	4	10	11	24	26	30	32	33	38	42	50	51	53	58	71	79	84	92												
	1			x				x				x					x		x														
	2		x	x	x														x														
	3				x		x	x	x			x				x	x											x	x				
	4				x				x							x			x									x	x				
	5		x	x									x			x		x										x	x				
	6		x	x	x											x												x	x				
	7				x																									x			
	8		x	x																								x	x	x	x		
	9			x																													
	10		x						x									x										x	x	x			
	11							x								x	x											x					
	12							x		x			x			x																	
	13															x														x			
	14		x					x		x				x		x	x			x	x	x											
	15																																
	16			x					x									x										x					
	17																	x	x											x			
	18																																
	19																																
	20																																
Pr (%)		44	56	68	77	58	47	67	55	57	58	55	77	60	67	72	76	90	88	88													

April

Rainfall Districts

	1	2	4	10	13	24	6	30	32	33	38	42	50	61	62	68	71	79	84	93
1	X	X	X			X		X		X			X			X		X		X
2	X	X	X		X				X		X	X			X	X	X			
3		X	X							X			X	X					X	X
4		X			X					X	X	X	X	X	X		X			
5	X	X	X					X	X	X			X	X	X	X				
6	X			X	X					X		X	X		X					
7									X	X		X	X						X	
8			X			X			X	X		X		X	X	X	X		X	X
9					X				X		X			X		X		X		
10										X		X								
11		X							X		X	X	X	X		X	X	X	X	X
12		X	X		X		X		X	X		X	X		X				X	
13										X				X						X
14					X				X	X		X	X		X					
15					X				X											
16									X	X			X			X				
17														X	X					
18										X			X							X
19								X						X		X	X	X		
20 (1)	85	83	83	14	72	28	18	60	91	37	64	87	93	87	79	87	69	44	77	45

May

Rainfall Districts

	1	2	4	10	13	24	6	30	32	33	38	42	50	61	62	68	71	79	84	93
1	X	X	X		X						X		X							X
2	X	X		X	X								X			X		X		
3	X	X	X				X	X					X							
4							X			X	X					X				X
5	X	X	X						X				X	X						
6	X	X								X		X	X					X		
7	X	X									X	X	X							
8						X		X	X		X			X		X				
9										X	X							X		X
10													X							
11	X	X			X							X	X				X			
12					X	X			X	X					X			X		
13	X					X			X				X	X	X		X			X
14	X	X		X					X	X	X				X	X	X	X		
15							X		X		X			X						
16			X							X		X								
17					X					X					X					
18	X	X				X					X					X				
19		X				X							X		X	X	X	X		
20 (1)	92	94	81	28	88	31	58	53	58	71	71	32	87	88	70	50	68	59	0	53

June

Rainfall Districts

	1	2	4	10	13	24	28	30	32	33	38	42	50	61	63	68	71	79	84	88
1		X	X									X								
2												X		X	X		X		X	X
3	X	X	X											X						
4	X	X										X		X	X		X		X	X
5					X		X	X	X			X		X	X				X	X
6					X	X	X	X	X			X		X		X	X	X	X	X
7															X					
8										X		X		X	X		X			X
9												X		X						
10									X				X				X			
11															X			X		
12					X							X			X					
13							X	X	X			X		X	X	X		X	X	X
14												X								X
15							X		X	X				X		X		X	X	X
16									X	X			X		X					X
17									X					X	X	X				
18												X			X					X
19		X		X	X				X	X					X					
Σ (%)	39	49	38	16	60	17	56	54	74	50	0	24	13	92	89	57	41	57	77	81

September

Rainfall Districts

	1	2	4	10	13	24	28	30	32	33	38	42	50	61	63	68	71	79	84	88
1		X		X	X		X			X	X	X								
2					X		X	X	X	X					X					
3	X	X	X			X									X	X	X			X
4					X	X														X
5					X	X	X							X						
6		X	X		X	X	X							X						
7					X		X	X	X		X			X	X	X		X		X
8					X	X	X											X		
9										X				X					X	
10									X					X	X					X
11					X				X	X										
12												X								
13						X	X	X												
14											X						X			X
15											X								X	X
16					X															
17	X					X	X	X					X							
18						X	X							X						
19					X	X	X	X									X			
Σ (%)	27	38	10	12	60	91	93	79	84	71	31	57	44	0	48	37	50	24	77	19

October

Rainfall Districts

	1	2	4	10	11	24	26	30	32	33	38	42	50	61	63	68	71	79	86	93
Principal Components																				
1																				
2																				
3																				
4																				
5																				
6																				
7																				
8																				
9																				
10																				
11																				
12																				
13																				
14																				
15																				
16																				
17																				
18																				
19																				
$R^2(\%)$	59	20	17	33	48	56	69	85	72	58	97	30	13	17	90	29	92	66	61	19

November

Rainfall Districts

	1	2	4	10	11	24	26	30	32	33	38	42	50	61	63	68	71	79	86	93
Principal Components																				
1																				
2																				
3																				
4																				
5																				
6																				
7																				
8																				
9																				
10																				
11																				
12																				
13																				
14																				
15																				
16																				
17																				
18																				
19																				
$R^2(\%)$	52	37	44	82	70	88	78	83	18	88	92	40	57	42	64	77	42	92	69	18

December

